We are IntechOpen,
the world's leading publisher of
Open Access books
Built by scientists, for scientists

6,900
Open access books available

185,000
International authors and editors

200M
Downloads

154
Countries delivered to

Our authors are among the

TOP 1%
most cited scientists

12.2%
Contributors from top 500 universities

BOOK CITATION INDEX
CLARIVATE ANALYTICS
INDEXED

WEB OF SCIENCE™

Selection of our books indexed in the Book Citation Index
in Web of Science™ Core Collection (BKCI)

Interested in publishing with us?
Contact book.department@intechopen.com

Stability and Flow Behavior of Fiber-Containing Drilling Sweeps

Matthew George[1], Ramadan Ahmed[1] and Fred Growcock[2]
[1]University of Oklahoma,
[2]Occidental Oil & Gas Corp.,
USA

1. Introduction

In the oil and gas industry, drilling sweeps are used to improve borehole cleaning when conventional drilling fluid fails to or is suspected of failing to sufficiently clean the wellbore. They are often applied immediately prior to tripping operations to clean the wellbore and reduce excessive annular pressure losses. The sweeps remove cuttings that cannot be transported to the surface during normal fluid circulation while drilling and provide additional vertical lift to the cuttings. Sweeps can be performed in all well inclinations from vertical to horizontal, as required by wellbore conditions. Drilling sweeps are an effective tool for counteracting poor hole cleaning, which can lead to an increase in non-productive time and costly drilling problems such as stuck pipe, premature bit wear, slow rate of penetration, formation fracturing, and high torque and drag (Ahmed & Takach, 2008).

Multiple field-tested techniques have been introduced over the years to prevent and reduce the proclivity of drilled cuttings to settle within the wellbore, therefore enhancing cuttings transport and improving hole cleaning. Previous studies indicate that cuttings transport in directional wells is dependent on fluid rheology, wellbore inclination angle, rotary speed of the drillpipe, flow rate, wellbore geometry, and other drilling parameters (Valluri et al., 2006). Considering these factors, the easiest and most economical procedures to improve hole cleaning involve increasing annular velocity preferably into the turbulent flow regime or using sweeps of higher density or viscosity than the drilling fluid. Sweeps are commonly categorized as i) high-viscosity; ii) high-density; iii) low-viscosity; iv) combination; and v) tandem sweeps (Hemphill, 2002). Sweeps provide a number of benefits such as reducing cuttings beds – thus decreasing annular pressure loss – and reducing torque and drag at the surface. Increasing the flow rate also provides the sweeps with extra lifting potential, though this must be closely monitored, as the details depend on the characteristics of the well. Pressure losses along the wellbore, as well as the equivalent circulating density (ECD), must be considered when designing and applying sweep fluids. Hole cleaning fiber added to the sweep fluid is thought to improve its performance with a negligible increase in viscosity and pressure loss (George et al., 2011). Previous studies (Marti et al., 2005; Rajabian et al., 2005; Guo et al., 2005) showed similar trends, with the apparent viscosity of fiber-polymer suspensions increasing linearly but slightly with increasing fiber concentration up to an approximate critical fiber concentration. At this critical concentration, the apparent

viscosity began to increase rapidly and exponentially with only small increases in fiber concentration. For field applications and for this study, fiber concentrations are maintained well below the critical threshold.

Reports from previous experimental studies (Ahmed & Takach, 2008) and field applications (Cameron et al., 2003; Bulgachev & Pouget, 2006) noted that adding a small amount of synthetic monofilament fiber (less than 0.1% by weight) improved solids transport and hole cleaning efficiency of the sweep over comparable non-fiber sweeps, with no noticeable change in fluid rheology. This favorable performance may be attributed to fiber-fiber and fiber-fluid interactions that create a stable network structure which can support cuttings. The fiber-fiber interactions can be in the form of direct mechanical contact and/or hydrodynamic interference among fiber particles. Mechanical contact among fibers improves the solids-carrying capacity of the fluid (Ahmed & Takach, 2008), while mechanical contact between the fibers and the cuttings beds helps to re-suspend cuttings deposited on the low side of the wellbore. As the fibers flow through the annulus, mechanical stresses develop between the fibers and settled cuttings. These mechanical stresses result in a frictional force which helps to re-suspend the cuttings, while the fiber networks carry the solids to the surface of the hole. Due to the fiber-fiber interaction, the bulk fiber network may move as a plug through the annulus. With the increased fluid velocity in the high side of the annulus, the fiber plug may move at a higher velocity relative to the local conditions at the low side of the annulus near the drillpipe. These fast moving fibers can transfer momentum to the deposited solids, overcoming the static frictional forces and initiating particle movement.

Although application of fiber suspensions in the oil and gas industry has been limited, they are common in other industries. Non-Brownian fiber suspensions have wide application in the pulp and paper industry, as well as in the manufacture of composite materials. These applications generally require uniform distribution of fiber particles throughout the suspending medium, which are often short and rigid and oriented parallel to the direction of motion or deformation. Similar to drilling fluid sweeps, these suspensions exhibit non-Newtonian characteristics such as the Weissenberg effect (Nawab & Mason, 1958; Mewis & Metzner, 1974), shear thinning (Goto et al., 1986), and viscoelasticity (Thalen & Wharen, 1964). The rheological properties of these non-Brownian fiber suspensions depend on the structure of the suspensions, which in turn is affected by features such as the fiber properties, interactions, suspending fluid properties, and the imposed flow field (Switzer & Klingenberg, 2003, 2004).

For drilling applications of fiber sweeps, some fiber flexibility is thought to be desirable, in order that the suspended fibers will not uniformly orient themselves while flowing up the wellbore annulus. In a sheared flow of highly-flexible, large-aspect-ratio fibers, the fibers flip, frequently collide with each other and the container walls, and orient themselves randomly. In fluids that contain a sufficient concentration of suspended fibers, the contacting, colliding fibers form heterogeneous structures, or networks, that flocculate and exhibit viscoelastic properties (Meyer & Wahren, 1964). Sozynksi & Kerekes (1988a,b) implicated mechanical contact as the principal mechanism in the formation of fiber "flocs." They suggested that fibers become locked in strained configurations due to their elasticity and frictional forces at fiber contact points, and referred to the fiber flocculation mechanism as "elastic fiber interlocking". A yield stress is also generated within the fiber suspension,

implying that a sufficient force must be applied to initiate flow (Meyer & Wahren, 1964). Bennington et al. (1990) measured the yield stress of various wood and nylon fiber suspensions. The yield stress (τ_y) measurements were directly influenced by volume fraction (Φ) as $\tau_y \sim \Phi^\beta$. The measured values of β varied with the fiber elasticity and aspect ratio, which was especially evident in comparisons between stiff wood fibers and relatively flexible nylon fibers. These frictional, or adhesive, contacts between fibers were believed to give rise to shear thinning behavior of suspensions of short nylon fibers in silicone oils at very low shear rates (Chaouche & Koch, 2001). This speculation is consistent with the idea that shear thinning arises when the torque associated with adhesive fiber-fiber contacts is comparable with the hydrodynamic torque rotating the gross flow of the particles. It may be noted that fiber flexibility (bending) and the base fluid's non-Newtonian behavior exert greater influence at high shear rates and with high-viscosity solvents, while fiber-fiber adhesion is most influential at low shear rates and with low-viscosity solvents (Chaouche & Koch, 2001).

Several studies have focused on simulating flexible fiber suspensions. Ross & Klingenberg (1997) modeled flexible fibers as inextensible chains of rigid prolate spheroids connected through ball and socket joints. This model can represent large aspect ratio fibers. Schmid et al. (2000) suggested that flexible fibers interact as chains of spherocylinders connected by ball and socket joints. This study also demonstrated that inter-fiber friction, even in the absence of attractive forces, can produce fiber flocculation (**Fig. 1**). While this and a subsequent study (Schmid & Klingenberg, 2000) were primarily concerned with the flow of non-Brownian fiber suspensions such as that thought to occur with pulp slurries in the paper-pulp industry, it is useful to understand the mechanisms which lead to flocculation. An important conclusion of those simulation studies (Schmid et al., 2000), which contradicts our work, is that fibers can flocculate when sheared. While this flocculation may enhance wellbore clean-up, the suspensions we tested generally dispersed when sheared and only flocculated under quiescent conditions when the fibers were allowed to separate and come together at the top of the vessel.
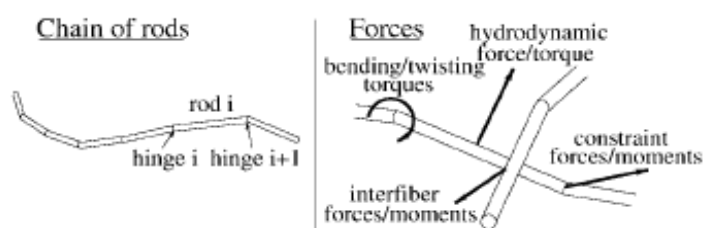

Fig. 1. Schematic of contacting fibers and forces (Schmid & Klingenberg, 2000)
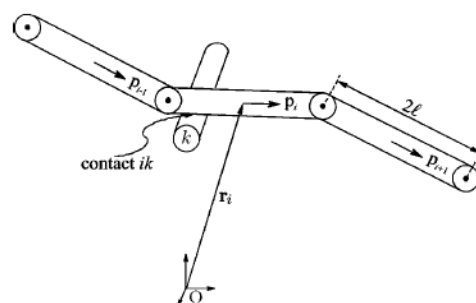
Fig. 2. Model of flocculated fiber particles that experience mechanical contact (Switzer & Klingenberg, 2003)

The fiber suspension modeling work was expanded by Switzer & Klingenberg (2003, 2004), who modeled flexible fiber suspensions as neutrally buoyant chains of linked rigid bodies immersed in a Newtonian fluid (**Fig. 2**). This model includes realistic features such as fiber flexibility, irregular shapes, and mechanical contact forces between fibers. The model also

considers curvature, that is the degree of sustained flexibility of a fiber particle, which is measured from a straight, rigid baseline form. The study re-affirmed the conclusion of the prior simulation studies that flocculation can arise from friction alone, in the absence of other forces, and that fiber flocculation increases with decreasing fiber curvature.

This study is concerned with the rheology of fiber-containing fluids specific to the oil and gas industry, and the propensity of the fiber to separate within the suspending medium, both of which provide insight into the flow behavior and effectiveness of fiber sweeps in the wellbore. The literature suggests that at critical concentrations, the fiber particles come into contact with each other and form networks. The strength of these networks depend on the prevailing fiber orientation and fiber flexibility. The non-rigid fiber particles dispersed and oriented randomly throughout the suspension provide the maximum opportunity for fiber entanglement, therefore increasing the cuttings resuspension and carrying capacity in the wellbore.

2. Rheology of fiber containing fluid

Controlling the rheology of the drilling and sweep fluids is essential to maintain favorable wellbore hydraulics and hole cleaning efficiency. This is of utmost importance when drilling extended and ultra-extended reach wells in deep water, where the slight difference between the formation fracture pressure and pore pressure requires a minimum overbalanced wellbore pressure condition. In such environments, the pressure and temperature ranges rise to levels that are difficult to emulate in laboratory experiments and predict precisely the rheology of the fluids downhole.

To predict the transport properties and performance of fiber sweeps under downhole conditions, the rheological properties of the base fluid and suspension must be understood. The proposed formulations for such fiber sweeps will be most effective when the rheology has been accurately modeled and fine-tuned for specific wellbore conditions. To begin to grasp how the fluid behaves, the relationship between shear stress and shear rate must be known. This is denoted as the shear viscosity profile, which is an aspect of the rheology of a fluid that is thought to control the hydrodynamics of flow. The most common shear viscosity models used in the oil and gas industry to characterize non-Newtonian drilling fluids include:

- Bingham-Plastic (BP): $\tau = YP + PV\,\gamma$
- Power Law (PL): $\tau = K\gamma^n$
- Yield Power Law (YPL) or Herschel Bulkley: $\tau = \tau_y + K\gamma^n$

where τ = shear stress at the wall, γ = shear rate, YP = yield point, PV = plastic viscosity, K = consistency index, n = fluid behavior index, and τ_y = yield stress.

As the drilling fluid must have sufficient cuttings-carrying capacity to keep cuttings from accumulating in the wellbore, the fluid must be capable of suspending the cuttings under quiescent conditions, i.e. its yield stress must exceed the settling velocity of the cuttings. The classic viscosity model used for drilling fluids is the Bingham-Plastic or viscoplastic model. Here the shear stress rises linearly with shear rate, with a slope given by PV. The intercept on the τ axis, YP, is often identified with the carrying capacity of the fluid but does not adequately describe the viscosity profile at very low shear rates. Most drilling fluids exhibit

a non-linear shear stress-shear rate relationship, which is best described by the Yield Power Law model. The YPL model is useful in describing a wide range of polymer-based, oil-based, and synthetic-based drilling fluids, from low shear rate to high shear rate. The yield stress (τ_y) defines the critical shear stress that must be reached before flow can initiate.

Recently, the shear viscosity profiles of synthetic-based drilling fluids were measured from 27°C to 138°C and from 1 bar to 346 bar (Demirdal et al., 2007). The study showed the viscosity to be extremely sensitive to downhole conditions, with the yield stress and consistency index drastically changing with temperature and pressure. The overall trend was that these parameters decreased with increasing temperature, and increased with increasing pressure. The evaluation also showed that the Yield Power Law model continued to describe adequately the shear stress-shear rate relationship over the entire range of temperature and pressure tested regimes. In another laboratory study (Yu et al., 2007), cuttings transport efficiency of drilling fluid was measured at elevated temperatures and pressures (up to 93°C and 138 bar). The experimental trend showed that higher temperatures diminished the cleaning efficiency of the fluid. Both of these studies suggest that as the fluid thins with increasing temperature, the amount of momentum transferred to the cuttings diminishes. The thinner fluid suspensions may exhibit a greater phase separation tendency, as it loses its ability to maintain a uniform fiber concentration while flowing in the annulus. This phase separation diminishes the quality of the hole cleaning provided by the fiber.

In designing a fiber-fluid formulation for wellbore cleaning sweeps, certain viscosity parameters can serve as indicators of how well the sweep will perform. The yield stress of the fluid represents the amount of force required to deform the fluid. At the same time, if the fluid possesses adequate yield stress to counteract the natural buoyancy of the fiber, the fiber may not separate. The yield stress may provide a good indication of how well the sweep will maintain uniformity when circulating up the annulus. However, the yield stress of the fluid does not tell the whole story, nor does shear viscosity itself provide a comprehensive portrait of the fluid. The elastic, extensional and thixotropic properties of the fluid very likely affect a fluid's ability to suspend and transport cuttings. Furthermore, in suspensions with sufficient fiber concentration, the fibers themselves can affect the fluid's rheology by forming networks in which each fiber maintains multiple contacts with adjacent fibers. These networks exhibit mechanical strength and viscoelastic behavior (Thalen & Wahren, 1964), which are controlled by the cohesive nature of the contact points (Switzer & Klingenberg, 2003). These cohesive forces are a result of the friction generated by normal forces at the contact points between elastically bent fibers (Kerekes et al., 1985). Soszynksi & Kerekes (1988a,b) proposed that these networks are the result of mechanical contacts, which are created due to "elastic fiber interlocking", a result of fiber elasticity and the fiber contact friction forces.

Multiple studies of the viscosity of fiber suspensions have reported the significance of fiber properties. Guo et al. (2005) showed that the rheological properties of fiber suspensions increased with increasing fiber volume fraction and fiber aspect ratio. These effects also increased with decreasing shear rate. Numerical simulations by Switzer & Klingenberg (2003) reported the strong influence that particle shape and inter-fiber friction have on the viscosity of fiber suspensions. The clustering of these suspensions also has a marked impact

on the viscosity: Chen et al. (2002) observed spikes in the shear stress-shear rate flow curves of fiber suspensions when they flocculated at low shear rates.
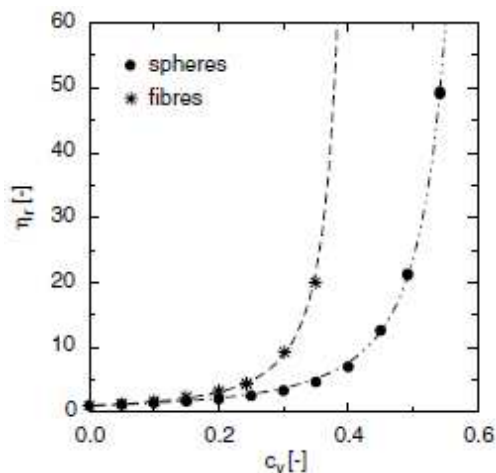

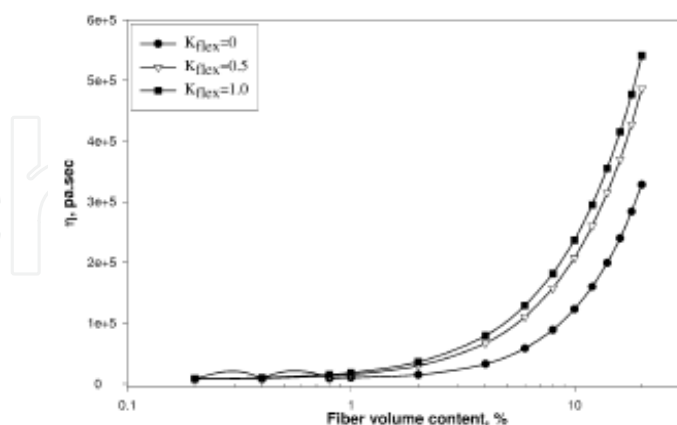Fig. 3. Suspension viscosity vs. concentration for spheres and fiber (Marti et al., 2005)

Fig. 4. Suspension viscosity vs. concentration for fibers of different flexibilities (Rajabian et al., 2005)

The ability of added fiber to improve hole cleaning without adversely impacting viscosity is the primary benefit in utilizing fiber sweeps. However, previous studies conducted on the viscosity of fiber suspensions (**Figs. 3 and 4**) have shown just how sensitive the fiber-fluid is to fluctuations in fiber concentration. Rajabian et al. (2005) investigated how the viscosity of fiber suspensions varied with increasing fiber concentration at varying degrees of fiber flexibility. In a similar study, Marti et al. (2005) looked into how the viscosity of suspensions of fibers and spheres, respectively, reacted with increasing particle concentration. While the data may not be highly correlated, both studies improve the basic understanding of the behavior of fibrous suspensions. The viscosity of the suspensions increases only slightly with increasing particle (fiber) concentration up to some threshold, above which it begins to increase rapidly and exponentially. These studies also indicated that the viscosity of the fiber-laden fluid is dependent on fiber flexibility and length. As observed in Fig. 4, the fibers with the highest degree of flexibility generated the highest viscosity at any given concentration.

This study focuses on identifying the behavior of fiber suspensions within the boundaries that are utilized in the oil and gas drilling industry. The scope of the experimental studies is limited to profiling the behavior and viscosity of a fiber suspension at concentrations not exceeding the upper practical limit at which this fiber has been used. This study will help to further verify the usefulness of fiber sweeps within the drilling industry.

2.1 Experimental investigations

Several base fluids were chosen to simulate the various drilling and sweep fluids utilized in the field (**Table 1**). A specially processed 100% virgin synthetic monofilament fiber was supplied for this research (**Table 2**), which was mixed with the base fluids at various concentrations of up to 0.08 % w/w.

	Base Fluid (kg / m³)	Weighting Agent	Fiber Concentration (%)
Water-Based Mud [WBM]	**XG** (1.00, 2.48, 4.99, 7.48)	None 998 kg/m³	0.00, 0.04, 0.08
	PAC (1.00, 2.48, 4.99, 7.48)	None 998 kg/m³	0.00, 0.04, 0.08
	XG / PAC [50%/50%] (1.00, 2.48, 4.99, 7.48)	None 998 kg/m³	0.00, 0.04, 0.08
	XG (2.48, 4.99, 7.48)	Barite 1438 kg/m³	0.00, 0.04, 0.08
	PHPA (0.49, 1.00, 1.49)	None 998 kg/m³	0.00, 0.04, 0.08
OBM	**Mineral Oil-base**	Barite 1462 kg/m³	0.00, 0.04, 0.08
SBM	**Internal-Olefin-base**	Barite 1450 kg/m³	0.00, 0.04, 0.08

Material	=	Polypropylene
Spec. Grav.	=	0.91
Length	=	10 mm (0.40 in)
Diameter	=	100 μm (0.004 in)
Melting Point	=	163°C – 177°C

Table 1. Test matrix of rotational viscometer measurements   Table 2. Fiber properties

The water-based fluids included those prepared with xanthan gum (XG) at two mud weights, polyanionic cellulose (PAC), partially hydrolyzed polyacrylamide (PHPA) and mixtures of XG and PAC. Formulations were prepared with a broad range of polymer concentrations. Two non-aqueous-based fluid systems were also tested: weighted mineral oil-based and internal olefin-based drilling fluids. These two fluid systems are designed and engineered to provide superior performance in locations not suitable for aqueous-based fluids. The rheology of these fluid systems are often adjustable, presenting the ability to custom-fit the fluid for certain environmental or in-situ conditions. Overall, the rheology of these fluid systems provide increased lubricity and yield stress over most conventional water-based fluids, but with reduced viscosity profiles. These characteristics can enable the fluids to prevent separation of the fiber within the suspension, and promote higher pump rates, both of which can reduce the size and occurrence of cuttings beds.

2.2 Experimental setup

The shear viscosity experiments were conducted using rotational viscometers (Chandler 35 and Fann 35A) with a thermocup. The Chandler 35 rotational viscometer has 12 speeds, and was modified to include a 1/5 spring. The weaker spring allows for more sensitive and accurate measurements in the low shear rate range and reports all shear stress dial readings 5x higher than their direct-reading counterparts. Both viscometers were calibrated and tested using multiple fluids to ensure readings were comparable.

2.3 Test procedure

The steps required to prepare the samples and record measurements are as follows:

Step 1. Preparation of Base Fluid: Bulk base fluid samples were prepared by mixing water, viscosifiers, and barite. Immediately after mixing, all water-based fluids were covered and left undisturbed for a minimum of 24 hours to ensure full hydration of

the polymers. Each fluid was then re-agitated, and a uniform sample was obtained to determine its specific gravity using a mud balance.

Step 2. **Preparation of Samples:** After the base fluids were mixed and hydrated (where necessary), fiber was added at weight concentrations of 0.02%, 0.04%, 0.06%, and 0.08%. For the unweighted water-based fluids, 0.08% w/w fiber concentration corresponded to 0.80 kg of fiber/1.0 m³ of suspension, whereas for the weighted (~1440 kg/m³) water-based and non-aqueous fluids it corresponded to approximately 1.14 kg of fiber/1.0 m³ of suspension (**Table 3**).

Step 3. **Viscometer Measurements at Ambient Temperature:** After all samples were prepared, the viscosity profiles of the base fluids were measured using two rotational viscometers (Chan 35 and Fann 35A). If the viscosity of the fluid being measured exceeded the spring capacity of the Chan 35, the Fann 35A was utilized for the higher shear rate measurements.

Step 4. **Viscometer Measurements at Elevated Temperature:** Samples were placed in an oven for heating. The oven was set at approximately 82°C, and samples were agitated every 15 minutes to ensure uniformity. Once a sample was heated to 77°C as confirmed by a mercury thermometer, the sample was removed from the oven and mixed for 30 seconds using a stand mixer. This mixing time was deemed adequate to achieve uniform re-dispersion of the fibers. Immediately after mixing, a portion of the sample was poured into the thermocup. Using a mercury thermometer, the thermocup temperature was adjusted to achieve a constant fluid temperature of 77°C. The viscometer measurements were taken using the procedure described in Step 3.

%		$\rho \approx 998$ kg/m³ (kg/m³)	$\rho \approx 1440$ kg/m³ (kg/m³)
0.02	=	0.20	0.29
0.04	=	0.40	0.57
0.06	=	0.60	0.86
0.08	=	0.80	1.14

Table 3. Equivalent fiber concentrations (% w/w) for different fluid densities

2.4 Experimental results

The shear stress of each fluid was measured at rotational speeds of 1 rpm to 600 rpm (1.7 to 1022 sec^{-1}) at ambient temperature and 77°C. Using the measured shear stress values, the apparent viscosity was calculated at each viscometer speed for all the fluids tested.

When circulating through the annulus, the fiber sweep is likely traveling in the plug flow regime. Therefore, the low shear rate range is more significant when analyzing and predicting the behavior of these fiber sweeps under downhole conditions. However, to provide a general understanding of fiber sweeps, **Figs. 5** and **6** show the results of the viscometer measurements for the entire shear rate range.

Although the experiments were conducted with four (4) levels of fiber concentration (Step 2), to reduce data clutter only the intermediate (0.04%) and high (0.08%) fiber concentrations were included in the figures for the water-based drilling fluids. A detailed analysis of the various fluids' shear viscosity parameters was previously conducted (George et al., 2011).

2.4.1 Effect of fiber concentration

One goal of the research is to determine the effect that adding fiber and increasing the fiber concentration has on the viscosity of the fluid. In essence, the fiber did not substantially affect fluid viscosity in any of these cases. This is consistent with a previous study (Ahmed & Takach, 2008) which found that adding fiber to drilling fluids had an insignificant effect on the fluid's flow behavior. According to field results and supporting theories previously stated, adding fiber to the fluid may improve the fluid's hole cleaning performance without affecting its viscosity, which suggests that other rheological properties dictate hole-cleaning performance.

For most of the water-based drilling fluids, the addition of fiber to the base fluid resulted in only a slight increase in apparent viscosity, while in a few cases, the apparent viscosity appeared to decrease. Though small, these differences are considered greater than the expected experimental uncertainty.

As an example of the water-based drilling fluid results, let us evaluate the experimental results of the high-temperature weighted XG polymer fluids (not shown). The fiber fluid mixed with 2.48 kg/m^3 XG polymer showed the most common effect observed in this work, namely that the apparent viscosity increased with increasing fiber concentration, especially at low shear rates. Conversely, the fiber fluid mixed with 4.99 kg/m^3 XG polymer shows an opposing trend, with fiber reducing apparent viscosity throughout the shear rate range measured. At the shear rate 51 s^{-1}, the difference in shear stress between the base fluid and 1.14 kg/m^3 fiber fluid is 15%.

The effect of fiber on viscosity was found to be relatively insignificant for the non-aqueous based drilling fluids (Fig. 6). Even at low shear rates, the fiber at the highest concentration tested increased the viscosity or shear stress at 51 s^{-1} by only 4% to 6% in most cases, and 8.8% in the most extreme case (Fig. 6a). This finding is encouraging, as fiber can be added to sweeps to enhance hole cleaning without fear of increasing the ECD. Oil-based and synthetic-based muds are often used in harsh, not-easily accessible environments where there is concern for shale interaction and environmental impact. Fiber sweeps might be employed to reduce the cuttings beds in these extended reach wells where pressure loss along the annulus is a major concern.

In every case, the addition of fiber appeared to have no impact on the general shape of the apparent viscosity vs. shear rate plots. The approximate viscosity model used for the base fluid appears to be acceptable for accurately describing the behavior of the fiber fluid, at least up to a temperature of 77°C.

In a study conducted by Ahmed & Takach (2008), the hole-cleaning efficiency of fiber sweeps was compared to that of the base fluid. The experiments were carried out in a flow loop with varying inclination angles, measuring the cuttings bed height and frictional pressure loss during sweep circulation. For the same annular velocity, the fiber sweeps generally showed a reduced bed height in the flow loop annulus. Annular pressure loss was recorded as a function of time for various flow rates. In most cases, the frictional pressure loss was approximately the same for the base fluid and fiber sweep. In one instance, however, the fiber sweep pressure loss was less than that exhibited by the base fluid. Pipe viscometer experiments were also conducted comparing flow curves of the base fluid and

fiber sweep. Viscometer pressure loss was measured as a function of flow rate. At low flow rates (laminar, plug flow regime), pressure loss for the base fluid and fiber sweep were equal, and the flow curves were similar.
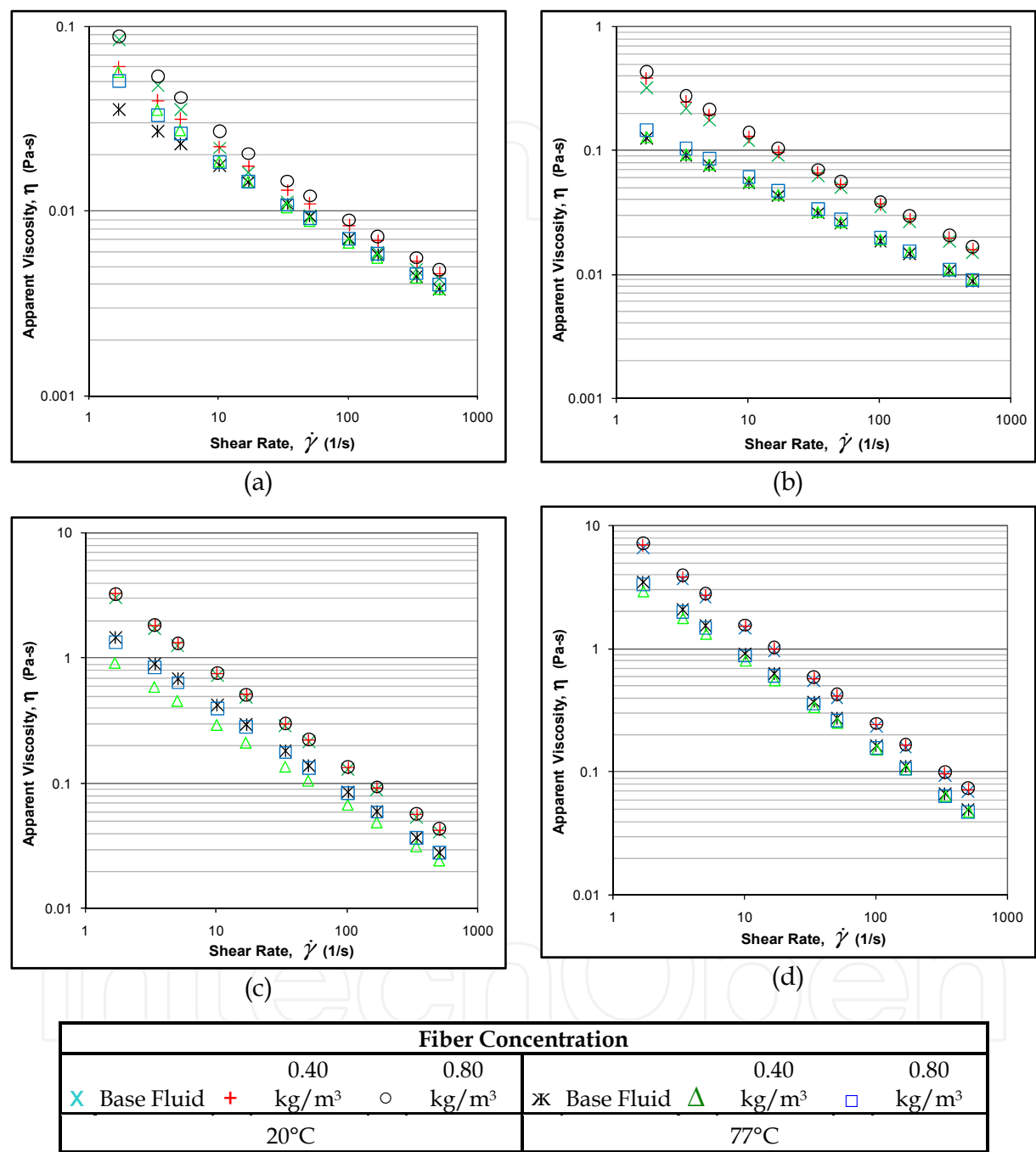

Fiber Concentration						
		0.40	0.80		0.40	0.80
X Base Fluid	+	kg/m³	○ kg/m³	⋇ Base Fluid △	kg/m³	□ kg/m³
20°C				77°C		

Fig. 5. Rheology of XG based fluid at 20°C & 77°C varying fiber & polymer concentrations: a) 1.0 kg/m³ XG; b) 2.48 kg/m³ XG; c) 4.99 kg/m³ XG; & d) 7.48 kg/m³ XG

2.4.2 Effect of temperature

In order to more closely approximate the behavior of the fiber fluid under downhole conditions, the ambient temperature experiments were repeated at a somewhat higher

temperature, as shown in Figs. 5 and 6. The general trend exhibited in all the fluids studied is that the fluid's ability to flow increases with temperature. The warmer temperature creates a "thinner" fluid that is more easily deformed and provides less resistance to flow.

As mentioned previously, adding fiber or increasing fiber concentration results in a slight general increase of the drilling fluid viscosity. In most cases, this same trend is observed in the elevated temperature measurements. However, in some fluids which exhibited an increase in viscosity at ambient temperature, no effect of fiber on viscosity was observed at the elevated temperature (Fig. 5b).

Fiber Concentration					
X	Base Fluid	+ 0.57 kg/m³	○ 1.14 kg/m³	ж Base Fluid	△ 0.57 kg/m³	□ 1.14 kg/m³
20°C			77°C		
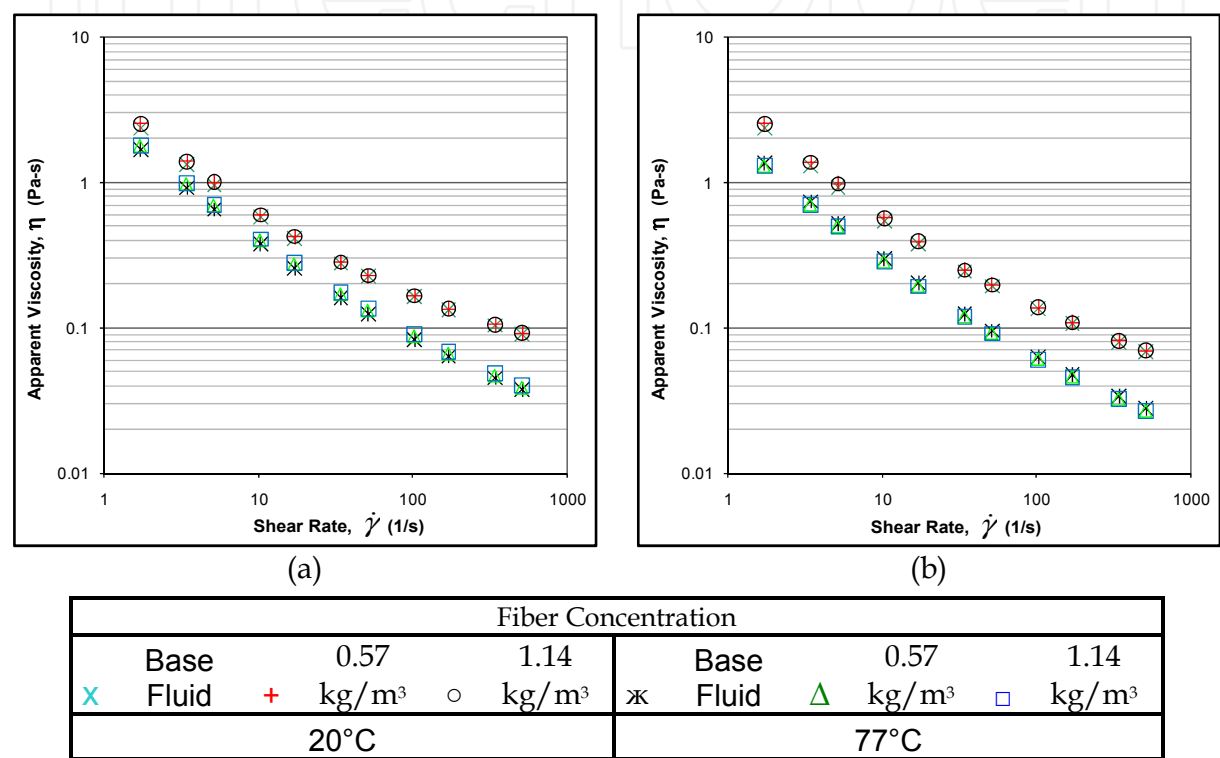
Fig. 6. Rheology of weighted fluids at 20°C & 77°C and varying fiber concentrations:
a) Oil-based mud (OBM), 1452 kg/m³; b) Synthetic-based mud (SBM), 1450 kg/m³

For the oil-based and synthetic-based muds, regardless of temperature, fiber has an insignificant influence on viscometric measurements. None of the water-based fluids tested showed this lack of effect over the entire shear rate range at both temperatures.

Although no experiments were carried out elevated pressure, other works have studied pressure effects on base fluid viscosity. Zhou et al. (2004) conducted experiments to investigate aerated mud cuttings transport in a HPHT (high pressure, high temperature) flow loop. The effect of elevated pressure (up to 35 bar) was found to have minimal influence on cuttings concentration. Another study (Alderman et al. 1988) investigated HPHT effects on water-based drilling fluid viscosity. The viscous behavior of the fluids at HPHT showed a weak pressure dependence and an exponential temperature dependence. It was also shown that the fluid yield stress was essentially independent of pressure, but highly influenced by temperature. Inasmuch as pressure has little effect on viscosity of the base drilling fluids, it is expected that pressure will have little effect on fiber-laden drilling fluids.

2.5 Conclusions

This study was conducted to investigate the effects of temperature and fiber concentration on the rheology of fiber-containing sweeps. Rotational viscometers were used to conduct rheology experiments at ambient and elevated temperature (77°C). From these experiments, shear stress values were recorded and subsequent apparent viscosity flow curves were created. The shear viscosity profiles of fiber sweep fluids were compared using graphical and curve-fitting regression analyses. Based on the experimental results and data analysis, the following conclusions can be made:

- The addition of fiber up to 0.08 wt % has a minor effect on the fluid's shear viscosity profile, whether at ambient or elevated temperature. Some instances showed slight increases in viscosity, while others showed a decrease with increasing fiber concentration.
- Increasing the temperature decreases the non-Newtonian behavior of the fiber fluid, and decreases the viscosity throughout the shear rate range of 2 to 1022 s⁻¹.
- In most cases, as fiber concentration increased, the viscosity showed slightly increasingly non-Newtonian behavior: in the Yield Power Law model, n decreased while τ_y increased.
- Neither oil-based nor synthetic-based fluids exhibited any significant shear viscosity sensitivity to fiber concentration at ambient or elevated temperature. It may be possible for OBM or SBM sweeps to be utilized in the field with no increase in ECD.

3. Stability of fiber-containing fluid

Very limited experimental work has been accomplished in the study of fiber-containing drilling fluids. In particular, there is a paucity of data concerning the behavior of these long-aspect-ratio fiber particles as they move within the drilling fluid. As mentioned previously, these multi-phase complex fluid systems must possess certain rheological properties to enable homogeneous distribution of the fibers throughout the bulk of the fluid to maximize shearing force on the cuttings beds and provide transport up the annulus.

In contrast to the manufacturing industry, where fiber suspensions are common, the conditions in drilling operations to which the sweep fluids are subjected can be severe. These adverse conditions require that the drilling fluids be stable to temperatures at a minimum of 120°C (some times as high as 250°C) and possess a density in the range of 200 to 2200 kg/m³. Most prior work on phase separation behavior of homogeneous, non-Brownian suspensions has been carried out with low-temperature, low-density fluids using particulates of density higher than the base fluid. In the case of drilling fluid fiber sweeps, the relative densities are reversed, as the specific gravity of the synthetic fiber is less than that of the base fluid. This relation encourages buoyancy, and the fibers tend to rise (separate) within the suspension. In spite of this difference, separation of fibers and fiber networks can be treated mathematically in a similar manner as settling of high-density particles.

The settling behavior of particles with density greater than the base fluid can be classified into four groups (Scholz, 2006):

- **Class I: Unhindered settling of discrete particles**. Non-interacting particles accelerate until a terminal settling velocity is reached, where the hydrodynamic drag and

gravitational force are balanced. Stokes' Law is commonly used to describe this motion of spherical particles.

- **Class II: Settling of a dilute suspension of flocculant particles**. Randomly moving particles collide and form aggregates (flocs) which behave as larger particles and have increased settling velocities compared to a single particle.
- **Class III: Hindered and zone settling**. Particle concentration is increased to a point where particles interact and form a loose network that displaces the liquid phase and gives rise to upward flow of liquid. This motion of the liquid reduces the overall particle settling velocity, and is called hindered settling. In large-surface-area settling applications with high particle concentrations, the entire suspension may tend to settle as a "blanket" (zone settling).
- **Class IV: Compression settling (compaction and consolidation)**. At even higher concentrations of particulates, e.g. at the bottom of a column containing a suspension, , a layer of sludge forms that becomes compressed over time and ultimately contains little or no liquid.

At low concentrations, unhindered "settling" (or more simply and generally "separation") can be applied to describe the motion of synthetic fibers. The modeling study considers Class I motion, which simply describes the forces and rising velocity of a single fiber suspended in a fluid. This prediction can be extrapolated to determine the rising velocity of a dilute suspension of fiber particles. Flocculation is not expected, since the fibers in this study are thought to be chemically inert. On the other hand, another mechanism may occur with fibers that is not possible for granular or spherical particles, namely entanglement. At sufficiently high concentration and with high-aspect-ratio flexible fibers, entanglement could occur and lead to behavior not unlike flocculation. Thus, Class I and a modified form of Class II could occur. Hindered/zone separation is not likely to be a factor due to the low concentrations of fiber. Nor is compression a plausible scenario for buoyant fibers, since there is no driving force for compaction of the fibers at the surface of the liquid, as there is for particles at the bottom of a fluid column.

The settling motion of a spherical particle is simple. The separation motion of a fibrous particle is much more complex (Qi et al., 2011). In the absence of extraneous forces, a sphere settles in a purely vertical direction. A cylindrical low-density flexible fiber suspended in a fluid can exhibit profligate behavior in three dimensions, as well as drift horizontally during its vertical ascent (Herzhaft & Guazzelli, 1999). The rising velocity of these fibers also depends on the fiber concentration, and how the particles orient themselves. Experimental studies investigating dilute and semi-dilute cylindrical or spheroid particles indicate that concentration is vital in understanding the phase separation (Qi et al., 2011; Kuusela et al., 2001, 2003; Koch & Shaqfeh, 1989; Herzhaft & Guazzelli, 1996, 1999). The overall consensus of these studies regarding the behavior of fiber suspensions is that fiber flocs separate faster than an individual fiber. However, as fiber concentration increases (independent of flocculation), the fibers exhibit hindered separation, and the separation velocity decreases below that of a single fiber.

These prior studies were concerned with phenomena of a similar nature to this work. This study focuses on rising velocities of fiber particles within a suspension, based on theoretical models and experimental results.

3.1 Modeling rising velocity of fiber particles

A mathematical model was developed to describe the effect of viscosity on the stability of fiber-containing drilling fluid sweeps. In order for the fiber to perform as efficiently and effectively as possible as a hole-cleaning aid, it is important that the fiber be homogeneously distributed throughout the base fluid, i.e. minimal separation of the fiber occurs under downhole conditions. Thus, a theoretical study was conducted to determine the desirable base fluid properties to formulate sweep fluids that are stable under downhole conditions.

For the sake of simplicity, our analysis only considers a single fiber suspended in the fluid (unhindered separation). This assumption ignores the effect of fiber-fiber interaction and fiber concentration. The analysis considers two orientations of the fiber: perpendicular to the direction of motion (horizontal orientation) and parallel to the direction of motion (vertical orientation). These orientations represent the boundaries within which the fiber can theoretically orient. However, it has been shown that a single fiber will orient itself horizontally (Kuusela et al., 2001, 2003; Qi et al., 2011). This stable orientation is not dependent on fluid velocity, and the fiber will eventually return to the horizontal position if acted upon by an outside force (Qi et al, 2011). Liu and Joseph (1993) investigated how a rigid slender particle is affected by liquid properties, particle density, length, and shape. They found that only particle concentration and the end shapes influenced particle orientation. This is consistent with studies by Herzhaft et al. (1996, 1999), which concluded that orientation of a settling spheroid is almost independent of aspect ratio but correlated to suspension concentration. As the fiber concentration is increased, the hydrodynamic interactions between the fibers will upset the stable horizontal fiber. With increasing fiber concentration, the fiber will show greater tendency to orient parallel to the direction of motion (Herzhaft et al.; 1996, Qi et al., 2011). By analyzing both cases, we can predict the rheological properties of the base fluid that can keep the fiber in suspension for a sufficient length of time.

To determine the velocity at which the submerged fiber particles move upward to the surface of the liquid, the sum of the forces in the vertical direction (y-axis) are set equal to zero. As shown in **Fig. 7,** the forces acting on the fiber moving within the column of fluid are buoyancy (F_b), hydrodynamic drag (F_D) and gravity (m·g). The projected surface area of a fiber particle, dependent upon particle orientation, is needed to compute the drag force. In this case, the fiber is horizontally oriented (perpendicular to the direction of motion of the fiber), and the generalized equation of the force balance in the vertical (y) direction is:

$$\sum F_y = F_b - F_D - mg = 0 \tag{1}$$

The forces acting on the fiber can be expanded as follows:

$$\sum F_y = V_p \rho_f g - \frac{1}{2} \rho_f C_{D,h} U_{p,h}^2 A_{p,h} - \rho_p V_p g = 0 \tag{2}$$

where $U_{p,h}$ is the rising velocity of the horizontally oriented particle. Rearranging the momentum balance equation to group similar terms:

$$\frac{1}{2} \rho_f C_{D,h} U_{p,h}^2 A_{p,h} = V_p \rho_f g - \rho_p V_p g \tag{3}$$

Both sides of Eqn. 3 are divided by ($\frac{1}{2}$ ρ_f) and the projected area for horizontal orientation ($A_{p,h} = L \times d$). Reducing like terms, expressing the fiber particle volume V_p explicitly ($\frac{1}{4}$ $\pi d^2 L$) and rearranging gives the formula for the particle rising velocity:

$$U_{p,h} = \left[\frac{\pi d g}{2} \left(\frac{\rho_f - \rho_p}{\rho_f} \right) \frac{1}{C_{D,h}} \right]^{\frac{1}{2}} \qquad (4)$$

A similar analysis for a vertically oriented particle with circular end area $\frac{1}{4}$ πd^2 gives

$$U_{p,v} = \left[2 L g \left(\frac{\rho_f - \rho_p}{\rho_f} \right) \frac{1}{C_{D,v}} \right]^{\frac{1}{2}} \qquad (5)$$

The drag coefficients (C_D) of the fiber particle must be estimated to predict the rising velocities using the above equations. Hole cleaning fibers are more or less straight and stiff and they can be considered long cylinders for the drag force calculation. Drag coefficient correlations and charts for long cylinders are well documented in the literature. For cylinders oriented perpendicular to the flow (i.e. cross flow), Perry (1984) presented a correlation (**Fig. 8**) that can be approximated with the equation given below.

$$Log(C_{D,h}) = \frac{0.9842 - 0.554 Log(\mathrm{Re})}{1 + 0.09 Log(\mathrm{Re})} \qquad (6)$$

This correlation is valid for Reynolds Number ranging from 10^{-3} to 1000. Due to the larger surface area of the horizontally oriented particle exposed to the direction of motion, the fibers moved at rates corresponding to very low Reynolds numbers. The Reynolds numbers in the lab experiments conducted here ranged from 10^{-17} to 10^{-3}.

The drag coefficient of a cylinder oriented in the direction of the flow is only a function of the aspect ratio (L/d). Based on available data in the literature (Hoerner, 1965), the following equation has been developed to estimate the drag coeffcieint C_{Dv}:

$$C_{D,v} = 0.825 + \frac{0.317}{1 + \left(\frac{l/d}{1.54} \right)^{4.23}} \qquad (7)$$

As shown in Eqn. (6), the drag coefficient of a cylindrical fiber under cross flow condition is a function of the Reynolds Number, which is generally expressed as Re = $\rho U_{p,h} d / \mu$ (i.e. the ratio of inertial force to viscous force). This definition holds true for Newtonian fluids, where shear stress $\propto$ shear rate. However, the fluids that are often utilized in fiber sweep applications are non-Newtonian. Hence, the Reynolds Number must be redefined using the apparent viscosity function as Re = $\rho U_{p,h} d / \mu_{app}$. The viscosity for Newtonian fluids is independent of the shear rate. However, for non-Newtonian fluids, the apparent viscosity varies with shear rate. Applying the Yield Power Law (YPL) rheology model, the apparent viscosity is expressed as:

$$\mu_{app} = K(\dot{\gamma})^{n-1} + \tau_y(\dot{\gamma})^{-1} \qquad (8)$$

The objective of this study was to determine the desirable Yield Power Law (YPL) fluid properties to keep the fiber in suspension in order to create efficient momentum transfer mechanisms between the sweep fluid and the cuttings bed. Only fluids with sufficient yield stress and/or low-shear-rate viscosity can be utilized to keep the fibers in suspension.
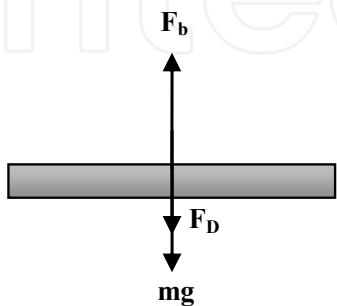

$$Log(C_{D,h}) = \frac{0.9842 - 0.554 Log(\text{Re})}{1 + 0.09 Log(\text{Re})}$$

Fig. 7. Free body diagram of a cylindrical particle rising in static fluid
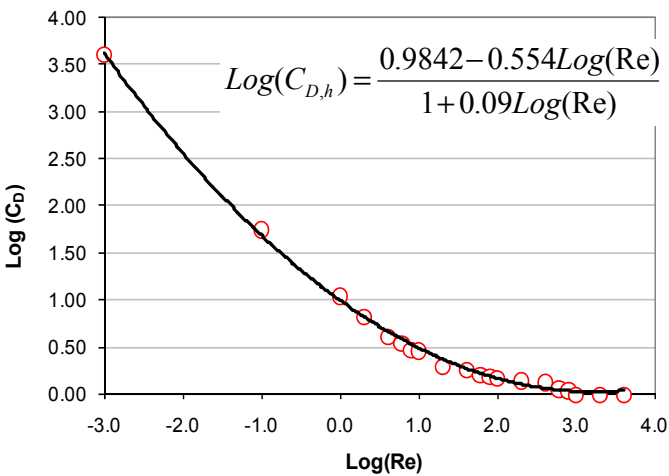
Fig. 8. Drag coefficient vs. Reynolds number for perpendicularly-oriented cylinders (Perry, 1984)

3.1.1 Non-rising particles under static conditions

In a static (quiescent) YPL fluid, a horizontally oriented cylindrical particle will not rise if the yield stress of the fluid is at least as high as its buoyancy (Dedegil, 1987). For a fully suspended particle, the momentum balance described by Eqn. (1) can be rewritten to include the static shear force acting on the particle in lieu of the drag force that is present under dynamic conditions. By taking a differential element of the cylindrical fiber, the vertical component of the maximum static shear stress (i.e., yield stress) acting on the fiber can be determined (**Fig. 9**). The direction of the shear stress acting on the cylinder depends on the location of the differential element as shown in Fig. 9. The stress acts on the area represented by the differential element shown in **Fig. 10**, which is expressed as:

$$dA = LRd\theta \qquad (9)$$

Then, the vertical component of the shear force acting on the differential element is:

$$dF_{shear} = dA \cdot \tau_y \sin\theta = LRd\theta \cdot \tau_y \sin\theta \qquad (10)$$

For a fiber-oriented vertically and horizontally, shear stresses act on the circumferential and end areas. However, the end areas are negligible when compared to circumferential area of the cylinder. This further simplifies the analysis. Neglecting the forces acting on the cylinder ends, the overall vertical component of the shear force is subsequently obtained by integrating Eqn. (10). After simplification, and considering that shear stress is exerted on opposing sides of the particle, the vertical component of the stress force acting on a horizontally oriented cylinder becomes:
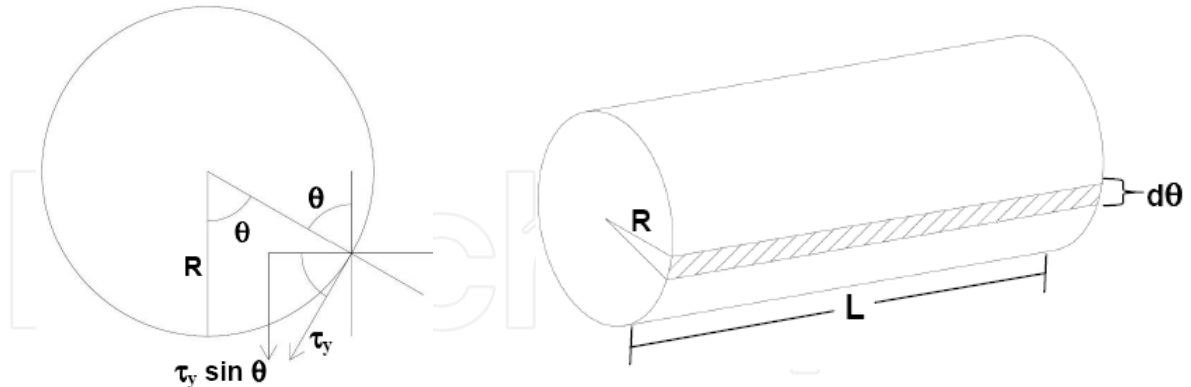
$$F_{s,h} = 2dL\tau_y \tag{11}$$

Fig. 9. Vertical component of shear force Fig. 10. Differential element of a cylinder subject to acting on a fully suspended cylinder shear force

The above equation predicts the maximum value of the shear force acting on the cylinder. For the sake of simplicity, the analysis is only concerned with a single fiber suspended in fluid. The cylinder is considered to be non-rotating and constantly perpendicular to the direction of motion of the fiber. In addition, as stated earlier, the calculations ignore fiber-fiber interactions, which would influence the momentum balance. The momentum balance equation can be written:

$$\sum F_y = 0 = V_p \rho_f g - 2dL\tau_y - \rho_p V_p g \tag{12}$$

Replacing the particle volume V_p with ($\pi d^2 L/4$), and grouping like terms results in:

$$2dL\left[\frac{\pi dg}{8}(\rho_f - \rho_p) - \tau_y \right] = 0 \tag{13}$$

For a fiber particle oriented in the vertical direction (**Fig. 11**), the shear force can be written as:

$$F_{s,v} = \pi d\tau_y \int_0^L dh = \pi dL\tau_y \tag{14}$$

Rewriting the force balance equation to include the shear force acting on a vertical oriented particle and grouping like terms results in:

$$\frac{\pi dL}{4}\left[dg(\rho_f - \rho_p) - 4\tau_y \right] = 0 \tag{15}$$

For this study, the dimensions of the fiber are known and fixed. Therefore, in order to determine the fluid property that can hold the fibers is suspension, Eqns. (13) and (15) must be rewritten to solve for critical shear stress as a function of density difference and fiber diameter for a fiber oriented horizontally and vertically, respectively. For a fiber oriented horizontally, the critical yield stress is:

$$\tau_{y,h} = \frac{\pi dg}{8}(\rho_f - \rho_p) \tag{16}$$

For a vertically oriented fiber particle, the critical yield stress is:

$$\tau_{y,v} = \frac{dg}{4}\left(\rho_f - \rho_p\right) \tag{17}$$

For this analysis, the fiber size and density are known. Thus, the critical yield stress is essentially a function of the fluid density, and increases linearly with density. **Fig. 12** shows the yield stress required to keep a vertically and horizontally oriented fiber particle (with properties given in Table 2)) from rising within the base fluid. For any given fluid density, horizontally (perpendicular) oriented fibers require greater yield stress to counteract the fluid's natural buoyancy. At the highest fluid density considered (2800 kg/m³), only a small yield stress (less than 0.72 Pa) is needed to keep the fiber in suspension. Eqns. 16 and 17 represent the relationship between the fiber's dimensions and density difference to the yield stress required to keep the fiber from rising.
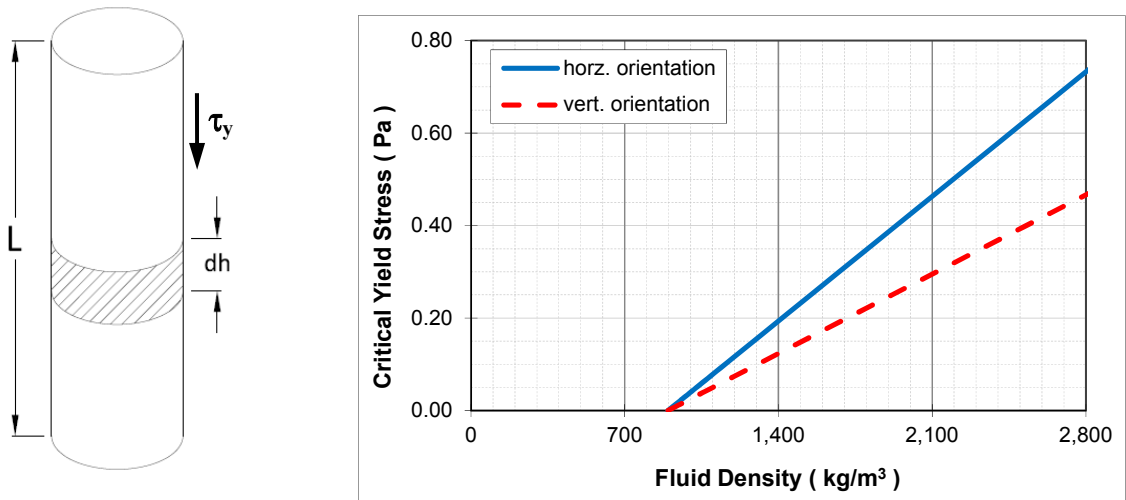
Fig. 11. Shear force acting on a vertically-oriented cylinder   Fig. 12. Critical yield stress as a function of fluid density for a non-rising particle

3.1.2 Non-rising particles under dynamic conditions

The models developed in previous sections are for fiber particles rising in a static fluid. They do not consider lateral motion and deformation of the fluid, as well as hydrodynamic diffusion effects. Eqns. (16) and (17) are appropriate for understanding rising behavior of fibers under static conditions. However, this study is to determine the hole cleaning efficiency of the fiber particles in real world situations such as fluid circulating up the annulus and drillstring rotation. The shearing motion of the fluid in the annulus will affect the apparent viscosity that subsequently influences the behavior of fiber particles in the base fluid. To accurately model the behavior of fiber under dynamic conditions, the overall shear rate must be computed from the primary and secondary flow shear rates, and the annulus is modeled as a narrow slot to obtain analytical solutions (**Fig. 13**).
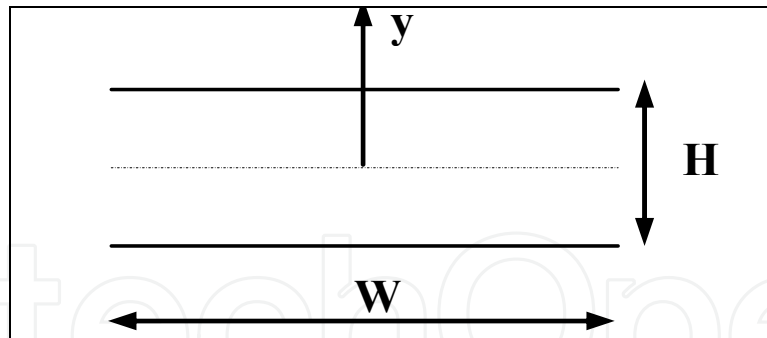
Fig. 13. Narrow slot representing annulus

As the sweep fluid is flowing in the annulus, it is subjected to primary and secondary flows. The primary flow is the gross flow of the fiber-fluid suspension in the annulus. For a fluid flowing in the annulus, the shear rate varies from zero to its maximum value, which occurs at the inner wall. Using the narrow slot approximation technique, the shear at any point in the annulus is given as (Miska, 2007):

$$\dot{\gamma}(y) = \frac{1}{K^n} \cdot \left[y \left(\frac{dp}{dL} \right) - \tau_y \right]^{\frac{1}{n}} \tag{18}$$

The above equation can be integrated to calculate the average shear rate as:

$$\dot{\gamma}_{ave} = \frac{1}{W(H/2)} \int_0^{H/2} \dot{\gamma}(y) W dy \tag{19}$$

For a YPL fluid, due to the presence of a plug zone, the average shear rate (i.e., primary share rate) calculation procedure is complex. However, in the plug zone the shear rate is zero and, therefore, can be neglected. For a power law fluid, Eqn. (19) yields:

$$\dot{\gamma}_{ave} = \dot{\gamma}_{primary} = \frac{1/K^n (dp/dL)^{1/n} (H/2)^{1/n}}{W(n+1/n)} \tag{20}$$

The slot width is W = π (d$_o$ + d$_i$)/2, and the clearance is H = (d$_o$ - d$_i$)/2. The primary shear rate is a function of flow geometry, properties of the fluid, and pressure gradient or annular velocity. The velocity gradient, or rising motion, of the particle induces the secondary flow, which is a function of the fiber particle rising velocity and the particle diameter:

$$\dot{\gamma}_{secondary} = \frac{U_p}{d_p} \tag{21}$$

Knowing that shear rate is the magnitude of the deformation tensor, the resultant shear rate scalar can be determined by the Eucledian norm:

$$\dot{\gamma}_{total} = \sqrt{\dot{\gamma}_{primary}^2 + \dot{\gamma}_{secondary}^2} \tag{22}$$

3.2 Modeling results

In order to predict the behavior of the fiber under dynamic conditions, the typical values of annular velocity and hydraulic diameter shown in **Table 4** were used. For a dynamic condition, the rising velocity of the fiber particle can be determined applying the rising velocity equations in combination with the resultant shear rate.

Fiber Diameter	=	0.0001 m	$D_{hydraulic}$	=	0.0889 m
Fiber Length	=	0.01 m	K	=	1.00 N-s^n/m^2
Fiber Density	=	897.04 kg/m^3	n	=	0.52
$U_{annulus}$	=	0.9144 m/sec			

Table 4. Input Data

To predict the possible results of the subsequent bench-top experiments, sensitivity analysis was conducted using the model. By varying certain properties of the fluids and determining the resulting rising velocities, the behavior of the fibers in suspension were investigated. For the sensitivity analysis, the rising velocity of a horizontally oriented fiber was determined under dynamic conditions varying the yield stress, fluid behaviour index "n", consistency index "K" and fluid density **(Figs. 14 and 15)**.

(a)   (b)
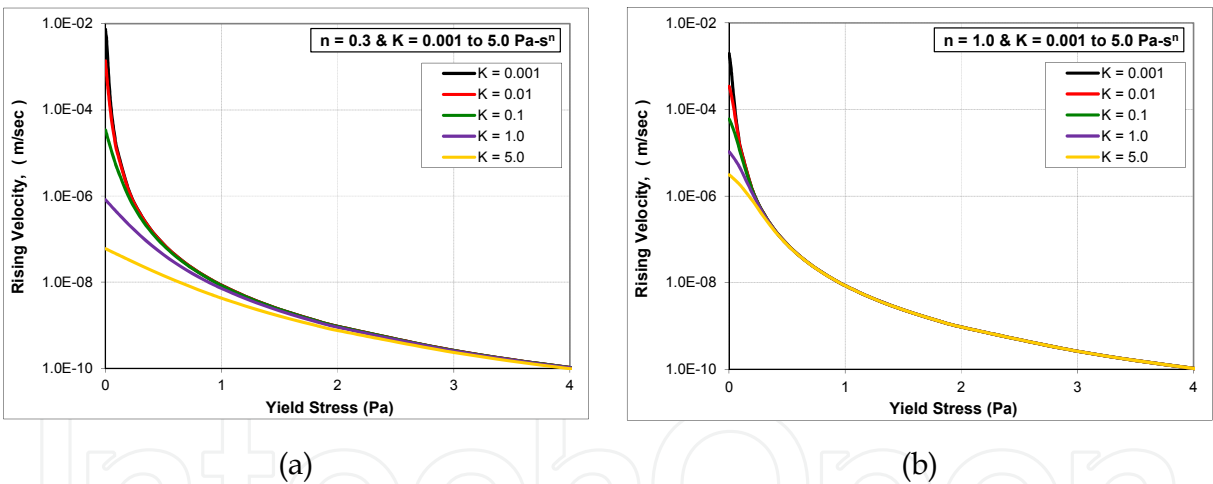
Fig. 14. Rising velocity vs. yield stress for horiz. oriented fiber in 998 kg/m^3 fluid
a) n = 0.3; and b) n = 1.0

The rising velocity of the fiber decreases as the consistency index increases and the fluid behavior index decreases. But these effects are relatively minor compared to yield stress and fluid density. The rising velocity decreases with increasing yield stress, as expected, and it decreases essentially in exponential fashion. Furthermore, with increasing yield stress, the consistency index term in Eqn. (8) becomes increasingly irrelevant in determining the Reynolds Number and has only a marginal effect on the rising velocity of the fiber. Like yield stress, fluid density has a strong effect on rising velocity. However, rising velocity decreases with decreasing fluid density, again decreasing in exponential fashion.
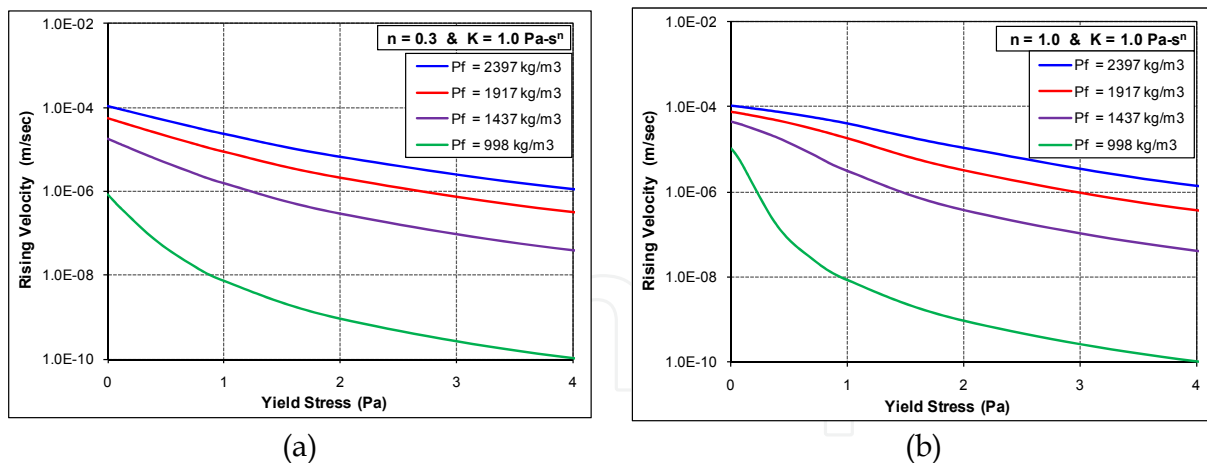
Fig. 15. Rising velocity vs. yield stress varying fluid density for horizontally oriented fiber particle, K = 1.0 Pa-s^n
a) n = 0.3; and b) n = 1.0

The yield stress and inherent "n" value of a specific fluid characterizes the degree to which the fluid behavior is non-Newtonian. Another trend worth investigating from Fig. 14 is the similarity of the rising velocity plots for different fluids with respect to their "n" values. It is observed that as "n" increasingly deviates from unity, the spread of the rising velocity plots at low yield stress values tends to increase. A careful examination of Fig. 14 reveals that the increase in the value of "n" substantially increases the rising velocity in fluids with high "K" values. Although this is unusual, analysis of Eqn. (10) shows that, at low shear rates (i.e., shear rates less than 1.0 s^{-1}), decreasing the values of "n" results in increased apparent viscosity.

To further explore the effect of yield stress on the upward motion of the fiber particles, the rising velocity of a horizontal fiber was determined as a function of yield stress, fluid density and "n" value. From Fig. 15, it can be seen that as the density of the fluid increases, the rising velocity increases. This is attributed to buoyancy, which increases as the difference in density between the fluid and fiber increases. This is consistent with the observation that the less dense fluids require smaller yield stresses to decrease the rising velocity or indefinitely suspend the fibers.

For a vertically oriented fiber particle, the rising velocity strictly relies on the fiber dimensions and density difference between the particles and the fluid. **Fig. 16** shows the effect of fluid density on the rising velocity of a vertically oriented fiber under dynamic conditions. This trend is similar to that observed for horizontally oriented fibers. As shown from Eqn. (7), when the fiber particle orients itself in the direction of motion, the drag coefficient becomes independent of the Reynolds Number and rheological properties of the fluid. Due to the high aspect ratio and low drag coefficient of the fiber, the rising velocity of a vertically oriented fiber particle is very high, and is about twice as high as when it is oriented perpendicular to the direction of motion (Herzhaft & Guazzelli, 1999). Although Koch & Shaqfeh (1989) found that a spheroid falls faster when its "thin" side is pointing in the direction of gravity, a single, unconstrained fiber will turn horizontal and oscillate around the stable horizontal orientation, separating slowly compared to vertical fibers (Kuusela et al., 2001, 2003; Qi et al., 2011). Due to the flexibility of the fiber and high

mechanical and hydrodynamic interferences, a vertical configuration is difficult to maintain, though it is preferred under dynamic conditions; therefore, predicted values do not reflect the actual rising speeds.
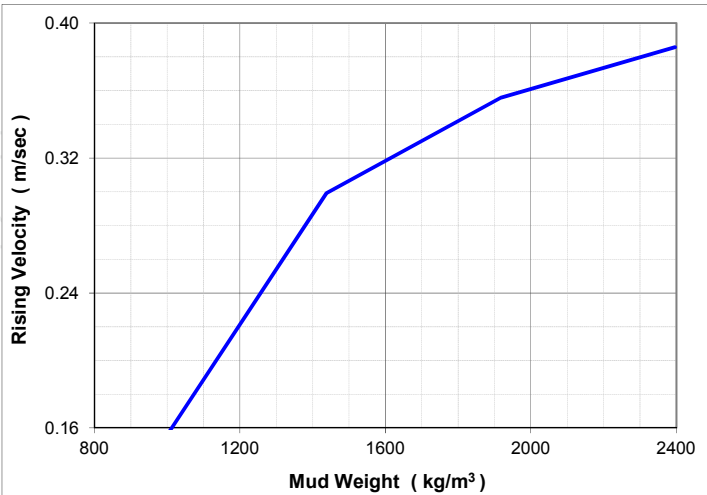

Fig. 16. Rising velocity vs. mud weight under dynamic conditions for vert. oriented fiber

3.3 Experimental study of fiber sweep stability

Several base fluids were chosen to simulate typical drilling and sweep fluids utilized in the field. The purpose of this investigation was to determine how well various base fluids would hold a fiber in suspension under ambient and elevated temperature conditions. The fibers used for these tests are described in Table 2. They have a specific gravity of approximately 0.91, which is less dense than the typical fluids in which they are suspended. Therefore, their natural tendency is to rise to the surface of the fluid and form fiber lumps. If the fibers rise while suspended in the fluid, the hole cleaning performance of the fluid diminishes and fiber lumps may plug some of the downhole tools. As discussed previously, fiber sweeps are mainly applied to minimize cuttings beds and reduce the concentration of cuttings in the wellbore. The fluids utilized for the sweep operations must possess properties conducive to maintaining a uniform fiber concentration throughout the bulk volume without increasing the ECD.

3.3.1 Experimental setup and procedure

Stability experiments were conducted using 250 mL graduated cylinders. Stand mixers were used to prepare the test fluid. Elevated temperature tests were carried out by heating test samples in a static oven. All fluids were prepared using the same process, unless otherwise specified by the fluids' respective product literature or laboratory preparation guidelines. Multiple polymeric fluids were tested, as well as oil-based and synthetic-based muds. Each polymeric fluid was prepared at the polymer concentrations shown in **Table 5**. The fluids and polymer concentrations utilized for this study were designed to simulate fluids used in drilling applications. **Table 6** lists the base % w/w concentration of the tested polymers, as well as their corresponding volumetric concentrations at different fluid densities.

	Base Fluid (kg / m³)	Weighting Agent	Fiber Concentration (%)
Water-Based Mud [WBM]	XG (1.00, 2.48, 4.99, 7.48)	None 998 kg/m³	0.00, 0.04, 0.08
	PAC (1.00, 2.48, 4.99, 7.48)	None 998 kg/m³	0.00, 0.04, 0.08
	XG / PAC [50%/50%] (1.00, 2.48, 4.99, 7.48)	None 998 kg/m³	0.00, 0.04, 0.08
	XG (3.59, 7.19, 10.78)	Barite 1438 kg/m³	0.00, 0.04, 0.08
	PHPA (0.49, 1.00, 1.49)	None 998 kg/m³	0.00, 0.04, 0.08
OBM	Mineral Oil-base	Barite 1462 kg/m³	0.00, 0.04, 0.08
SBM	Internal-Olefin-base	Barite 1450 kg/m³	0.00, 0.04, 0.08

%		$\rho \approx 998$ kg/m³ (kg/m³)	$\rho \approx 1440$ kg/m³ (kg/m³)
0.05	=	0.49	0.72
0.10	=	1.00	1.44
0.15	=	1.49	2.16
0.25	=	2.48	3.59
0.50	=	4.99	7.19
0.75	=	7.47	10.78
1.20	=	11.98	17.26

Table 5. Test matrix for stability experiments

Table 6. Equivalent polymer concentrations

The process used for preparing the water-based fluids followed these steps:

Step 1. **Preparation of Base Fluid**: The fluid samples were initially mixed with tap water in bulk using a stand mixer to begin hydration of the polymer. Hot water was used to accelerate the hydration time. The polymeric fluids were then placed in a blender and mixed for 30 minutes, and left to sit for 24 hours to ensure complete hydration.

Step 2. **Sample Preparation**: After sitting static for 24 hours, the fluids were re-agitated using a stand mixer to ensure uniformity of the samples. The bulk fluid was then divided into 300-mL samples (**Fig. 17**). Fiber was added to the samples by volumetric concentration in increments of 0.20, 0.40, 0.60, and 0.80 kg/m³ for unweighted, water-based fluid (approx. 0.02%, 0.04%, 0.06%, and 0.08% by weight for 998 kg/m³ mud, see Table 3).
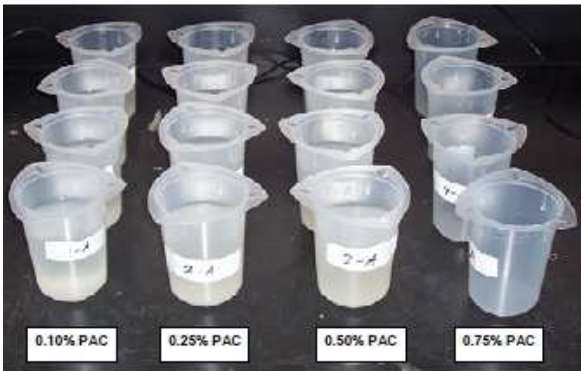

Fig. 17. Fluid samples organized by polymer and fiber concentration (George et al., 2011)
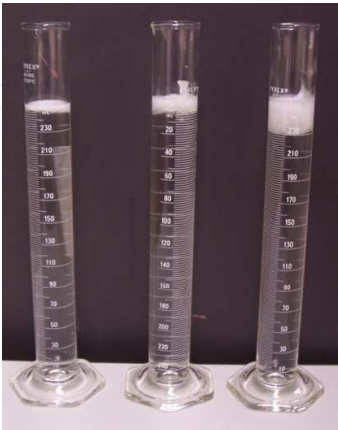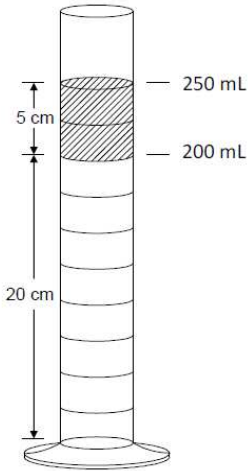
Fig. 18. Unstable test fluids after 1.0 hour test

Fig. 19. Graduated cylinder used for stability experiment

Step 3. **Heating the Samples**: The samples were placed in the oven for approximately 10 minutes to preheat the fluid. They were removed from the oven and re-agitated with the stand mixer to ensure fiber uniformity. The fluid samples were then immediately transferred to 250-mL graduated cylinders, and placed in the oven for one hour.

Step 4. **Extracting the Fiber**: The graduated cylinders were promptly removed from the oven after one hour. Under quiescent conditions, buoyant fiber particles move toward the surface of the sample, increasing the fiber concentration near the surface of the liquid. In unstable fluids, most of the fiber particles reached the surface of the sample (**Fig. 18**) after one hour. Using a 60 cc syringe, an aliquot of the top 50 mL of the fluid (**Fig. 19**) was removed from each cylinder and placed in a beaker. Water and surfactant were mixed in with the fiber-fluid to aid in cleaning the fibers.

Step 5. **Weighing the Fiber**: The fibers were separated from the fluid using a screen, and remixed with water and surfactant to further clean the fibers. The fibers were then screened again, dried in an oven, and weighed.

3.4 Experimental results

The experiments were designed to look at the effects of fluid viscosity profile on rising velocity. For the water-based drilling fluids, the viscosity was varied by using different types and concentrations of polymers, as well as barite. The primary purpose of the barite is to control density, but it also affects viscosity. For the oil-based and synthetic-based drilling fluids, the viscosity profiles and density were varied solely by using barite. The stability of the fiber-fluid suspension was tested for various fluids at varying polymer concentration. A few stability experiments were also conducted at ambient temperature, but with essentially the same qualitative results. The tests were conducted with no shear applied to the fluid, so the only shear present was exerted by the fiber itself as it moved upward in the fluid. The fluids tested are shear-thinning, so that apparent viscosity decreases with increasing shear rate. Under downhole conditions with the fluid circulating up the annulus, the viscosity may be considerably lower than under static conditions.

3.4.1 Effect of base fluid rheology on stability of fiber sweep

Visual observations during the tests showed the formation of three fluid layers within the graduated cylinder: clear layer on the bottom, uniform concentration layer in the middle and fiber accumulation layer on top. As the fiber particles migrate, the clear layer with a distinct boundary forms at the bottom. In the absence of hindered separation, the boundary is expected to move upward at a constant velocity, same as the rising velocity of the particles. At the same time, the accumulation layer develops at the top. As particles continuously migrate from the bottom to the top, the concentration and thickness of the accumulation layer increases. Assuming initial uniform fiber dispersion throughout the entire test specimen, the fiber volume of the top layer is equivalent to 20% of the total fluid column. Therefore, the change in average concentration of the top layer can be used to quantify the level of instability in the fluid system. Applying a mass balance for the solid phase, the average fiber concentration at a given time (t) can be estimated as:

$$c(t) = \frac{\left(U_{p,h} * c_f * A_c * t\right) + \left(V_c * c_f * 20\%\right)}{V_c * 20\%} \tag{23}$$

where A_c and V_c are the cross-sectional area and volume of the cylinder, respectively. For a completely unstable fluid, all fibers will raise to the top layer, and the final concentration will be five times greater than the initial concentration.

Figs. 20 to 25 show the test results along with model predictions. The results are presented in terms of final fiber concentration of the top layer as a function of initial fiber concentration. In the plots, the unstable fluid line illustrates the maximum fiber concentration that would occur in the top layer if all the fiber particles migrate into this layer. The stable line shows the initial fiber concentration in the top layer that does not change with time because of complete stability. The results complement the viscosity profiles measured previously for these fluids. The fluids that possess yield stress generally showed greater stability. Xanthan gum (XG), a very common drilling fluid, exhibited expected behavior (Fig. 20a). All except the 0.10% XG fluid showed complete stability.
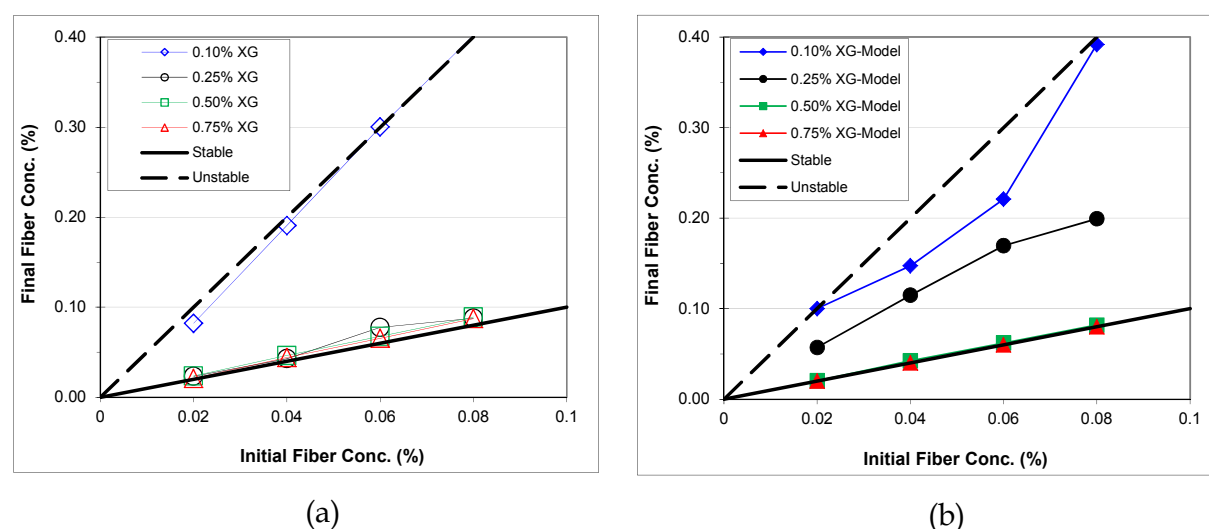

Fig. 20. One-hour stabilities of XG based fiber sweep at 77C: a) Lab experiment; b) Mathematical model

The PAC polymeric fluid showed no stability at 77°C (Fig. 21a). PAC is typically used as a fluid loss additive, not for its cuttings carrying capacity. However, the solution remains clear when mixed with water, and is a good tool for observing the fibers in suspension. In an attempt to determine if the PAC fluid had any potential as a fiber suspension fluid at 77°C, the duration of the experiment was shortened to 30 minutes. In this short amount of time, the fiber in the thicker fluid had not yet migrated to the surface, while the thinner fluids once again showed no stability. The PAC fluid mixed at 0.25% w/w fiber showed unexpected stability, but it appeared to be caused by an artifact. Upon visual inspection, the fiber appeared to have grouped in the middle of the cylinder, preventing the majority of the fiber from rising to the top part of the cylinder. The hydrodynamic and mechanical effects between the container wall and the rising fibers caused the formation of a fiber plug (lump) that did not move. This phenomenon persisted for the length of the experiment. Upon slight perturbation of the cylinder with the fiber-fluid, the fiber plug fell apart and the fiber rose to the surface in a matter of minutes.
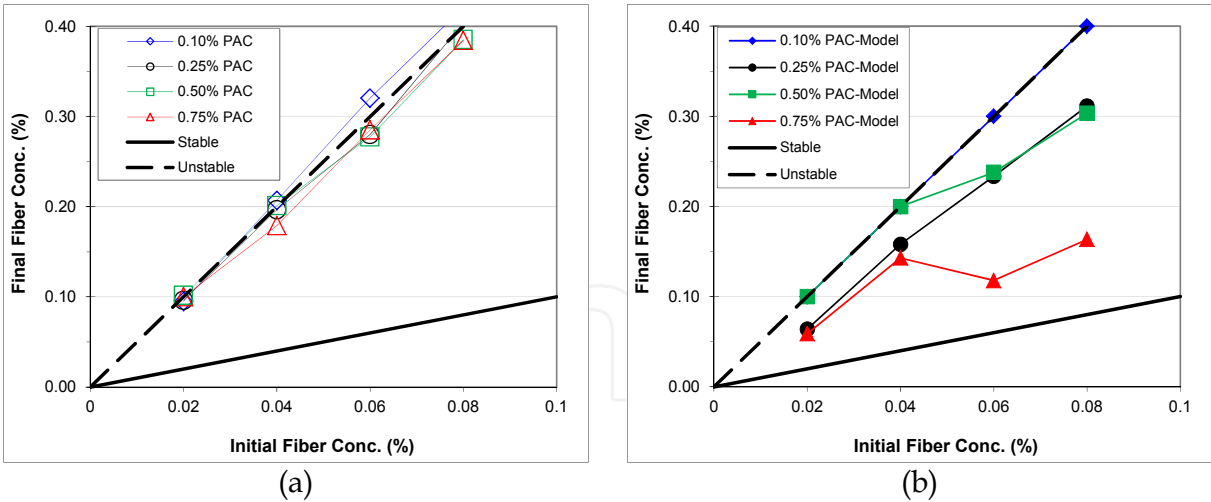
Fig. 21. One-hour stabilities of PAC based fiber sweeps at 77°C: a) Lab experiments;
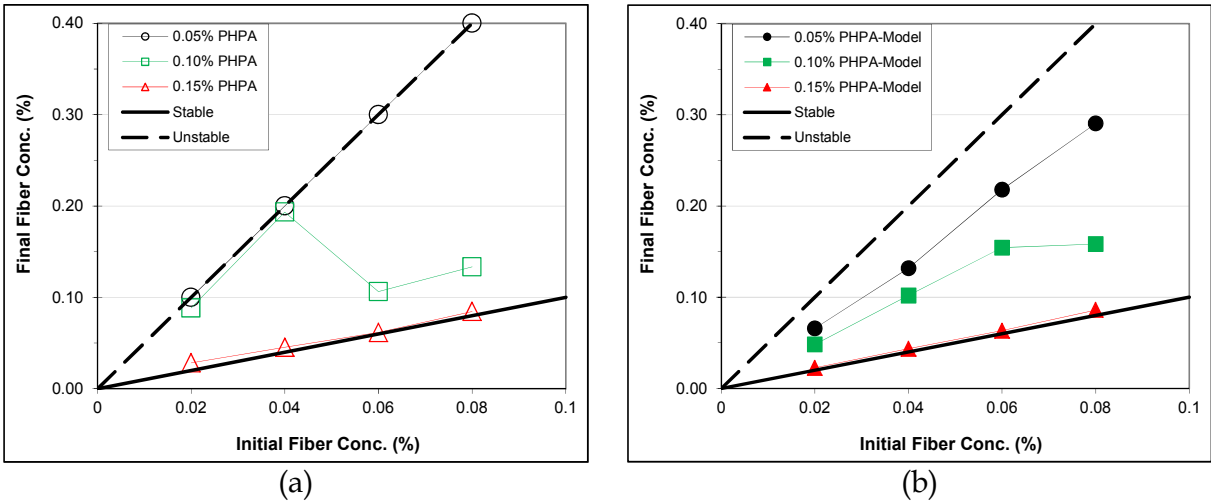b) Mathematical model

Fig. 22. One-hour stabilities of PHPA based fiber sweeps at 77°C: a) Lab experiments;
b) Mathematical model

Another clear fluid tested during the experiments was Partially Hydrolyzed Polyacrylamide (PHPA), which is often utilized as a shale stabilizer in drilling applications. When used at concentrations commonly used in the field, the thickest fluid (0.15% PHPA) showed stable behavior (Fig. 22a) while the thinner fluid (0.05% PHPA) became unstable. The intermediate viscosity fluid (0.10% PHPA) was essentially unstable, too. At high fiber concentrations, the experimental results showed stable behavior, but this is probably attributable to the formation of a fiber plug, as in the case described above for PAC. Another polymer tested was a 1:1 blend of XG and PAC, which was pursued to determine whether the combination of these two would provide as much stability as XG alone. The two thicker fluids exhibited stability, while the two thinner fluids did not (Fig. 23a). Thus, the blend did not perform as well as pure XG, and the addition of XG resulted in an opaque fluid, so that visual clues to the mixed fluid's stability were absent.

Drilling fluids are usually weighted in order to control formation pressure and support the borehole wall. Weighting is usually carried out through the addition of a weighting agent like

barite. As the fluid density is increased, so does the density difference between the fluid and the fiber, which increases the buoyancy force. It is expected that this in turn will increase the rising velocity of the fiber. On the other hand, increasing the concentration of weighting material usually results in an increase in viscosity, including the yield stress. Figs. 24 and 25 depict the results of the weighted fluid stability experiments. Despite the increased buoyancy force acting on the fiber particle, the experiments showed that the weighted fiber fluids were just as stable as the unweighted ones (ref **Fig. 20**), evidently because the viscosity increase of the weighted fluid kept pace with the density increase. The weighted and unweighted oil-based mud (OBM) and synthetic-based mud (SBM) demonstrated similar stability behavior (Fig. 25). In these two fluid systems, increasing the density by the addition of barite had no detrimental effect on the stability of the suspension. The fluids are formulated to provide properties advantageous to drilling applications. They exhibit relatively low overall viscosities but have sufficient yield stress to prevent the fibers from rising.
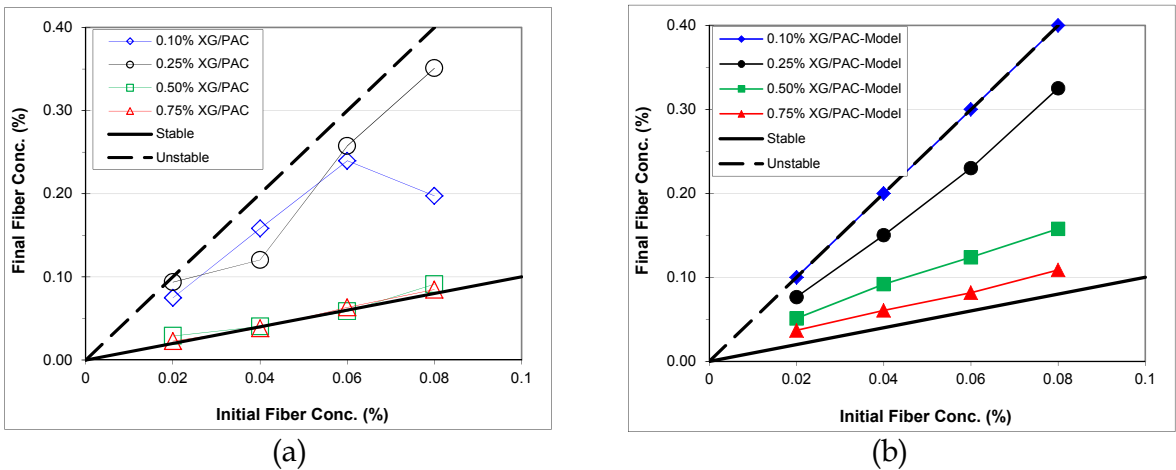

Fig. 23. One-hour stabilities of XG/PAC based fiber sweeps at 77°C: a) Lab experiments; b) Mathematical model
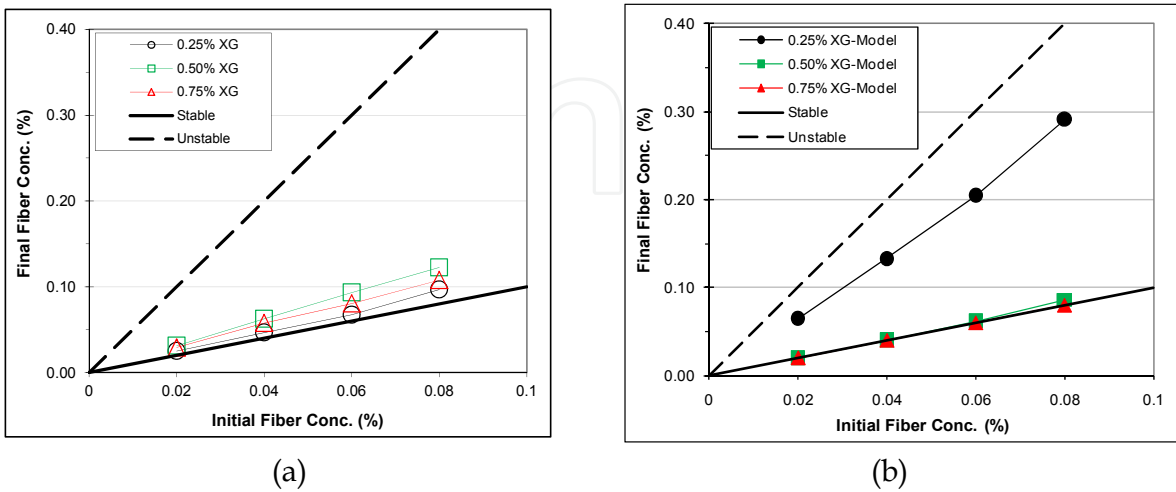

Fig. 24. One-hour stabilities of XG based weighted (1438 kg/m³) fiber sweeps at 77°C: a) Lab experiments; b) Mathematical model
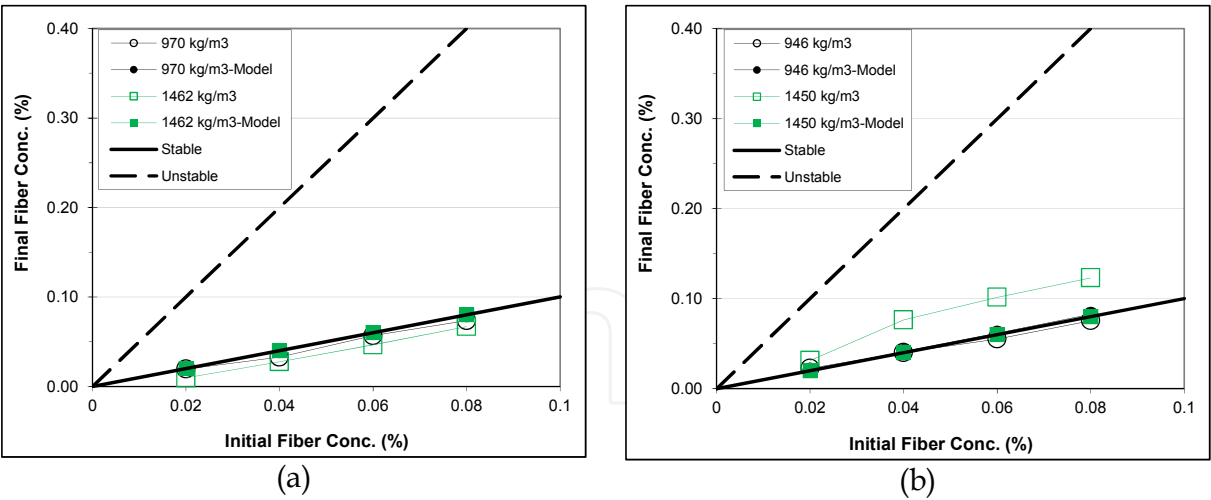
Fig. 25. Measured and predicted one-hour stability of non-aqueous based fluids at 77°C:
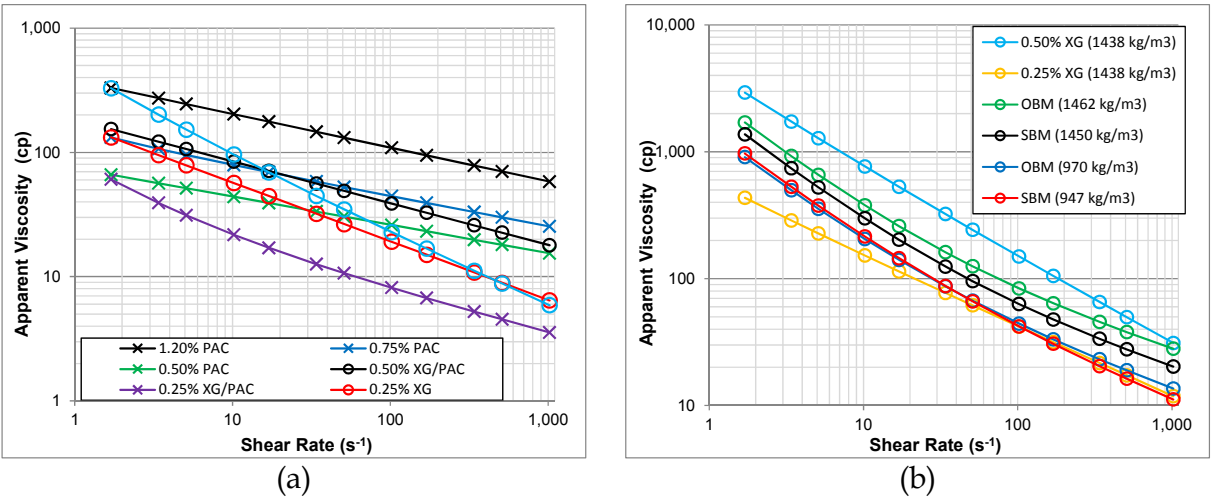a) Oil-based mud (OBM); b) Synthetic-based mud (SBM)

Fig. 26. Apparent viscosity vs. shear rate of water and non-aqueous based fluids at 77°C:
a) Low-viscosity fluids; b) High-viscosity fluids

Intuitively, the magnitude of the fluid's resistance to deformation or viscosity should provide a good indication of its internal ability to resist flow. Therefore, an increase in a fluid's viscosity would result in an increase in the ability to hold particles in suspension. As it pertains to the current study, an increase in polymer concentration generally results in higher viscosity, which in turn should yield a more stable fiber suspension. Visual observation of the fluids while mixing can also provide insight into the fiber fluid's probable stability. The rheological study on fibrous fluids that was undertaken previously was reconciled with the stability experiment results to compare the apparent viscosities of the stable and unstable fluids (**Fig. 26**). Fig. 26a shows a few low viscosity fluids, some of which were unstable. This data contradicts the original hypothesis that the fluid's viscosity or rheological properties would determine its ability to maintain stability. Easily apparent is the viscosity profile of the 1.20% PAC fluid, overall the most viscous fluid present in the figure. Despite its relatively high viscosity, this fluid was unstable (Fig. 26a). Also present in this figure are three stable fluids (0.25% XG, 0.50% XG/PAC, and 0.15% PHPA). It is

important to note that these fluids exhibited lower apparent viscosity at low shear rate than the 1.20% PAC fluid. The 0.25% XG fluid even exhibited lower viscosity than the 0.75% PAC fluid, which was also unstable.In general, XG based fluids showed lower fiber rising velocities than other polymeric fluids. Xanthan Gum polymer may have a structure than can easily tangle with the fiber particles. Fig. 26b depicts various stable high-viscosity fluids that were tested, including invert emulsion OBM and SBM.. With a dispersed phase (i.e., water phase) ranging from 20% to 30%, the OBM and SBM exhibit strong structure that can hinder the movement of fiber particles. Therefore, even though rheological properties play a great role in maintaining the fiber in suspension, other properties of the fluid such as the type of polymer and the presence of fluid structure may have some influence on the ease with which fiber fluids undergo phase separation.

3.4.2 Effect of temperature on stability of fiber sweep

As stated previously, most of the experiments were carried out at 77°C, though a few were conducted at ambient temperature (20°C). As expected, most of the suspensions tested at ambient temperature showed essentially no separation of the fiber. At elevated temperature, however, most of the fluids showed some instability. Although this effect of temperature appears to be associated with viscosity, the influence of temperature declines as the fluids becomes more viscous and increasingly non-Newtonian in nature.

3.5 Comparison of model predictions with experimental results

The rising velocity model presented in Section 3.1 was developed to predict the stability of fiber suspensions and determine fluid properties necessary to prevent the separation of fibrous particles. These models take into account various forces acting on each individual particle while suspended in the fluid, such as the buoyancy force created by the difference between fiber and fluid density,. The model was formulated to predict rising velocities for particles oriented horizontal and vertical. This was done to simulate the two extreme cases of particle orientation within the fluid. The rheological parameters of the fluids obtained from viscometric measurements are inputs into both models to compare model predictions with the actual experimental measurements. As the tested fluids exhibit non-Newtonian behavior, the rising velocity of the fiber particles becomes a function of rheological parameters of the fluid, which were determined in Section 2.4. The Yield Power Law (YPL) model is a suitable constitutive equation for describing the majority of drilling fluids currently used in the industry. From the viscometric measurements, the parameters of the test fluids were determined using regression analysis and used in the models. By determining the distance the fiber particles rise in one hour and the amount of fiber that entered into the top layer in that period, we were able to estimate the final concentrations of the top layer. Model predictions shown from Figs. 20 to 25 were obtained using the horizontal orientation model. These results generally compare favorably with the test results. However, in some cases discrepancies are apparent, especially with PAC-based fluids. This indicates that some other measure of the internal structure of fiber-laden fluids is lacking.

The predictions of the vertical orientation model were also compared with fiber separation measurements, but the results did not compare favorably. Indeed, that model predicted all

fluids to be unstable, which contradicts the experimental results wherein many of the fluids proved to be relatively stable. When comparing the two mathematical models, the dimensional terms differ. For both models, the area projected to the fluid flow depends on the orientation of the fiber. If the fiber is oriented perpendicularly (horizontally) to the flow, its rectangular profile (length x diameter = 1.0×10^{-6} m^2) provides the governing dimensions, whereas for vertical orientation the profile is the circular end area ($\frac{1}{4}$ π d^2 = 7.85×10^{-9} m^2). However, geometry of the projected area only partially explains the difference in results. The drag coefficient (C_D) is also different for the two cases. C_D is inversely proportional to rising velocity, as it counteracts the buoyancy force. For a vertically oriented particle, drag force resisting the rising fiber is exclusively related to the fiber aspect ratio (Hoerner, 1965), independent of the fluid properties. Conversely, for a horizontally oriented particle, the drag force is implicitly related to the Reynolds Number (Perry, 1984). The rather large aspect ratio in comparison to the rectangular projected area and fluid property dependency results in a vertically oriented particle rising velocity that is anywhere from three to five orders of magnitude higher than that for horizontally oriented particles.

Fluid density is one of the controllable model parameters that has a marked influence on the stability of fiber sweeps. However, operationally this is dictated by wellbore stability issues. Rising velocity is a direct function of the difference between fluid density and particle density. However, the increased viscosity associated with weighted fluid hinders settling of the barite particles For instance, the model prediction for the stability of the weighted XG based fluids (Fig. 24b) shows both favorable and unfavorable results, while the experimental results indicated stable fluids with a slight departure from complete uniformity for the two thicker fluids. With its current formulation, the model considers a single particle rising in the fluid. It does not account for the hindering effect of barite particles.

The oil-based and synthetic-based muds (Fig. 25) showed remarkable stability, both experimentally and mathematically. Both the weighted and unweighted OBM and SBM exhibited high yield stress, and all fiber-fluid combinations tested showed stable behavior. This was reinforced with the mathematical model predictions of similar results.

3.6 Conclusions

This study was undertaken to investigate the stability of fiber sweeps at ambient and elevated temperature conditions. Experiments were conducted using different base fluids (several water-based and non-aqueous fluids) with varying fiber concentrations. Fibers were extracted from the samples after the test and weighed to determine the final fiber concentration in the top layer. This data was used to determine if the fiber had risen while in the fluid sample, or if uniformity had persisted throughout the length of the experiment. These measurements were compared with stability predictions obtained from the mathematical model. After analyzing and comparing all the data to date, the following inferences can be made:

- Horizontally oriented particle model predictions are in general concurrence with the experimental data, and reasonable real-time application performance can be predicted using the model. The vertically oriented particle model overestimates rising velocity of fibers in all fluids tested, which does not reflect experimental results and is not expected to provide accurate predictions.

- Despite the dominant effect of fluid viscosity on the phase separation of fiber sweeps, other properties of the fluid such as elasticity and extensional viscosity should be examined.
- Selecting the type of polymer used for drilling sweep applications is critical in designing fluids that have good stability under downhole conditions. XG polymer appears to be a better choice than PAC or PHPA.
- Oil-based and synthetic-based fluids possess high resistance to separation of fibers from the base fluids. This could be attributed to the high yield stress that they exhibit and the presence of internal structure perhaps associated with their invert emulsion character.

4. Nomenclature

A_c = Cross-sectional area (m²)
$A_{p,h}$ = *Projection area of horizontally oriented particle (m²)*
$A_{p,v}$ = *Projection area of vertically oriented particle (m²)*
BP = Bingham Plastic
c = *Average fiber concentration*
$C_{D,h}$ = *Drag coefficient for a horizontally oriented particle*
$C_{D,v}$ = *Drag coefficient for a vertically oriented particle*
c_f = *Initial fiber concentration*
d = *diameter of fiber particle (m)*
d_i = *inner diameter of annulus (m)*
d_o = *outer diameter of annulus (m)*
D_h = *hydraulic diameter, $d_o - d_i$ (m)*
ECD = Equivalent circulating density
F_B = *Buoyancy force (N)*
F_D = Drag force (N)
F_{shear} = Shear force (N)
g = gravitational acceleration
K = Consistency index (Pa-sⁿ)
L = Fiber particle length (m)
N = Flow behavior index
n = Fluid behavior index
OBM = Oil-based mud
PAC = Polyanionic Cellulose
PHPA = Partially-Hydrolyzed Polyacrylamide
PL = Power Law
R = Radius (m)
R^2 = Coefficient of Determination
Re = Reynolds Number

V_p = Volume of fiber particle (m³)
XG = Xanthan Gum
YPL = *Yield Power Law*
s = second
SBM = Synthetic-based mud
t = time
$U_{p,h}$ = *Rising velocity of horizontally oriented particle (m/s)*
$U_{p,v}$ = *Rising velocity of horizontally oriented particle (m/s)*

Greek Letters

$\dot{\gamma}$ = shear rate (s⁻¹)
$\dot{\gamma}_{ave}$ = Average shear rate (s⁻¹)
$\dot{\gamma}_{primary}$ = Primary shear rate (s⁻¹)
$\dot{\gamma}_{secondary}$ = Secondary shear rate (s⁻¹)
$\dot{\gamma}_{total}$ = Total shear rate (s⁻¹)
θ = Angle
μ = Fluid viscosity (Pa-s)
μ_{app} = Apparent fluid viscosity (Pa-s)
ρ = density (kg/m³)
ρ_f = fluid density (kg/m³)
ρ_P = particle density (kg/m³)
τ = Shear stress (Pa)
τ_y = Yield stress (Pa)
$\tau_{y,h}$ = Critical yield stress of horizontally oriented particle (Pa)
$\tau_{y,v}$ = Critical yield stress of vertically oriented particle (Pa)

5. References

Ahmed, R.M. & Takach, N.E. 2008. Fiber Sweeps for Hole Cleaning. Paper SPE 113746 presented at the SPE/ICoTA Coiled Tubing and Well Intervention Conference and Exhibition, The Woodlands, Texas, 1-2 April.

Alderman, N.J., Gavignet, A., Guillot, D. & Maitland, G.C. 1998. High-Temperature, High-Pressure Rheology of Water-Based Muds. Paper SPE 18035 presented at the SPE Annual Technical Conference and Exhibition, Houston, Texas, 2-5 October.

Bennington, C.P.J., Kerekes, R.J., & Grace, J.R. 1990. The Yield Stress of Fibre Suspensions. *Can. J. Chem. Eng.* 68 (5): 748-757

Bivins, C.H., Boney, C., Fredd, C., Lassek, J. Sullivan, P., Engels, J., Fielder, E.O. et. al. 2005. New Fibers for Hydraulic Fracturing. *Schlumberger Oilfield Review* 17 (2): 34-43.

Bulgachev, R.V. & Pouget, P. 2006. New Experience in Monofilament Fiber Tandem Sweeps Hole Cleaning Performance on Kharyaga Oilfield, Timan-Pechora Region of Russia. Paper SPE 101961 presented at the SPE Russian Oil and Gas Technical Conference and Exhibition, Moscow, Russia, 3-6 October.

Cameron C. 2001. Drilling Fluids Design and Management for Extended Reach Drilling. Paper SPE 72290 presented at the IADC/SPE Middle East Drilling Technology conference, Bahrain, 22-24 October.

Cameron, C., Helmy, H., & Haikal, M. 2003. Fibrous LCM Sweeps Enhance Hole Cleaning and ROP on Extended Reach Well in Abu Dhabi. Paper SPE 81419 presented at the SPE 13th Middle East Oil Show and Conference, Bahrain, 5-8 April.

Chaouche, M. & Koch, D.L. 2001. Rheology of non-Brownian Rigid Fiber Suspensions with Adhesive Contacts. *J. Rheol.* 45 (2): 369-382

Chen, B, Tatsumi, D., & Matsumoto, T. 2002. Floc Structure and Flow Properties of Pulp Fiber Suspensions. *J. Soc. Rheol., Jpn.* 30 (1): 19-25

Dedegil, M.Y. 1987. Drag Coefficient and Settling Velocity of Particles in Non-Newtonian Suspensions. *Journal of Fluids Engineering* 109 (3): 319-323.

Demirdal, B., Miska, S., Takach, N.E. & Cunha, J.C. 2007. Drilling Fluids Rheological and Volumetric Characterization Under Downhole Conditions. Paper SPE 108111 presented at the SPE Latin American and Caribbean Petroleum Engineering Conference, Buenos Aires, Argentina, 15-18 April.

Drilling Fluid Rheology. 2001. Kelco Oil Field Group, Houston, Texas (Rev. Sep 2005).

George, M.L., Ahmed, R.M. & Growcock, F.B. 2011. Rheological Properties of Fiber-Containing Drilling Sweeps at Ambient and High Temperature Conditions. Paper AADE-11-NTCE-35 presented at the AADE National Technical Conference & Exhibition, Houston, Texas, USA, 12-14 April.

Goto, S., Nagazono, H., & Kato, H. 1986. The Flow Behavior of Fiber Suspensions in Netwonian Fluids and Polymer Solutions. I. Mechanical Properties. *Rheologica Acta* 25 (2): 119-129

Guo, R., Azaiez, J., & Bellehumeur, C. 2005. Rheology of Fiber Filled Polymer Melts: Role of Fiber-Fiber Interactions and Polymer-Fiber Coupling. *Polymer Eng. and Sci.* 45 (3): 385-399.

Hemphill, T. & Rojas, J.C. 2002. Drilling Fluid Sweeps: Their Evaluation, Timing, and Applications. Paper SPE 77448 presented at the SPE Annual Technical Conference and Exhibition, San Antonio, Texas, 29 September-2 October.

Herzhaft, B., Guazzelli, E., Mackaplow, M., & Shaqfeh, E. 1996. Experimental Investigation of a Sedimentation of a Dilute Fiber Suspension. *Phys. Rev. Lett.* 77 (2): 290-293

Herzhaft, B. & Guazzelli, E. 1999. Experimental Study of Sedimentation of Dilute and Semi-Dilute Suspensions of Fibres. *J. Fluid Mech.* 384: 133-158

Hoerner, S.F. 1965. *Fluid-Dynamic Drag; Practical Information on Aerodynamic Drag and Hydrodynamic Resistance.* Midland Park, New Jersey: Hoerner Fluid Dynamics

Koch, D. & Shaqfeh, E. 1989. The Instability of a Dispersion of Sedimenting Spheroids. *J. Fluid Mech.* 209: 521-542

Kuusela, E., Hofler, K., & Schwarzer, S. 2001. Computation of Particle Settling Speed and Orientation Distribution in Suspensions of Prolate Spheroids. *J. Eng. Math.* 41 (2-3): 221-235

Kuusela, E. & Lahtinen, J. 2003. Collective Effects in Settling of Spheroids Under Seatdy-State Sedimentation. *Phys. Rev. Lett.* 90 (9): 1-4

Liu, Y.J. & Joseph, D.D. 1993. Sedimentation of Particles in Polymer Solutions. *J. Fluid Mech.* 255: 565-595

Maehs, J., Renne, S., Logan, B. & Diaz, N. 2010. Proven Methods and Techniques to Reduce Torque and Drag in the Pre-Planning and Drilling Execution of Oil and Gas Wells. Paper SPE 128329 presented at the IADC/SPE Drilling Conference and Exhibition, New Orleans, Louisiana, 2-4 February.

Majidi, R. & Takach, N. 2011. Fiber Sweeps Improve Hole Cleaning. Paper AADE-11-NTCE-36 presented at the AADE National Technical Conference & Exhibition, Houston, Texas, USA, 12-14 April.

Marti, I., Hofler, O., Fischer, P. & Windhab, E.J. 2005. Rheology of Concentrated Suspensions Containing Mixtures of Spheres and Fibres. *Rheologica Acta* 44 (5): 502–512.

Metzner, A.B. & Reed, J.C. 1955. Flow of Non-Newtonian Fluids – Correlation of the Laminar, Transition, and Turbulent-flow Regions. *A.I.Ch.E. Journal* 1 (4): 434-440.

Mewis, J. & Metzner, A.B. 1974. The Rheological Properties of Suspensions of Fibers in Newtonian Fluids Subjected to Extensional Deformations. *J. Fluid Mech.* 62 (3): 593-600

Meyer, R., Wahren, D. 1964. On the elastic properties of three-dimensional fibre networks. *Sven. Papperstidn.* 67: 432-436

Miska, S. 2007. Advanced Drilling, Course Material, University of Tulsa.

Nawab, M.A. & Mason, S.G. 1958. The Viscosity of Dilute Suspensions of Thread-Like Particles. *J. Phys. Chem.* 62 (10): 1248–1253

Perry, R.H. & Green, D.W. 1984. *Perry's Chemical Engineering Handbook. 6th Edition.* Japan: McGraw-Hill.

Power, D.J., Hight, C., Weisinger, D. & Rimer, C. 2000. Drilling Practices and Sweep Selection for Efficient Hole Cleaning in Deviated Wellbores. Paper SPE 62794 presented at the IADC/SPE Asia Pacific Drilling Technology conference, Kuala Lumpur, Malaysia, 11-13 September.

Qi, G.Q., Nathan, G.J., & Kelso, R.M. 2011. Aerodynamics of Long Aspect Ratio Fibrous Particles Under Settling. Paper AJTEC2011-44061 presented at the ASME/JSME 8th Thermal Engineering Joint Conference, Honolulu, Hawaii, USA, 13-17 March.

Rajabian, M., Dubois, C., & Grmela, M. 2005. Suspensions of Semiflexible Fibers in Polymeric Fluids: Rheology and Thermodynamics. *Rheologica Acta* 44 (5): 521–535.

Ravi, K.M. & Sutton, D.L. 1990. New Rheological Correlation for Cement Slurries as a Function of Temperature. Paper SPE 20449 presented at the SPE Annual Technical Conference and Exhibition, New Orleans, Louisiana, 23-26 September.

Robertson, N., Hancock, S., & Mota, L. 2005. Effective Torque Management of Wytch Farm Extended-Reach Sidetrack Wells. Paper SPE 95430 presented at the SPE Annual Technical Conference and Exhibition, Dallas, Texas, 9-12 October.

Ross, D.F. & Klingenberg, D.J. 1997. Dynamic Simulation of Flexible Fibers composed of Linked Rigid Bodies. *J. Chem. Phys.* 106 (7): 2949-2960

Schmid, C.F. & Klingenberg, D.J. 2000. Mechanical Flocculation of Flowing Fiber Suspensions. *Phys. Rev. Lett.* 84 (2): 290-293

Schmid, C.F., Switzer, L.H., & Klingenberg, D.J. 2000. Simulations of Fiber Flocculation: Effects of Fiber Properties and Interfiber Friction. *J. Rheol.* 44 (4): 781-809

Scholz, M. 2006. *Wetland Systems to Control Urban Runoff.* Amsterdam, The Netherlands: Elsevier.

Sozynksi, R.M. & Kerekes, R.J. 1988a. Elastic Interlocking of Nylon Fibers Suspended in Liquid. Part I. Nature of Cohesion Among Fibers. *Nord Pulp Paper Res. J.* 3: 172-179

Sozynksi, R.M. & Kerekes, R.J. 1988b. Elastic Interlocking of Nylon Fibers Suspended in Liquid. Part II. Process of Interlocking. *Nord Pulp Paper Res. J.* 3: 180-184

Swerin, A. 1997. Rheological Properties of Cellulosic Fibre Suspensions Flocculated by Cationic Polyacrylamides. *Colloids Surf. A: Physicochem. Eng. Aspects* 133 (3): 279-294

Switzer, L.H. & Klingenberg, D.J. 2003. Rheology of Sheared Flexible Fiber Suspensions via Fiber-Level Simulations. *J. Rheol.* 47 (3): 759-778

Switzer, L.H. & Klingenberg, D.J. 2004. Flocculation in Simulations of Sheared Fiber Suspensions. *Intl. J. Mult. Flow* 30 (1): 759-778

Thalen, N. & Wahren, D. 1964. Shear Modulus and Ultimate Shear Strength of Some Paper Pulp Fibre Networks. *Sven. Papperstidn.* 67 (7): 259-264

Valluri, S.G., Miska, S.Z., Ahmed, R.M. & Takach, N.E. 2006. Experimental Study of Effective Hole Cleaning Using "Sweeps" in Horizontal Wellbores. Paper SPE 101220 presented at the SPE Annual Technical Conference and Exhibition, San Antonio, Texas, 24-27 September.

Xu, A.H. & Aidun, C.K. 2005. Characteristics of Fiber Suspension Flow in a Rectangular Channel. *Intl. J. Multiphase Flow* 31 (3) 318–336.

Yamamoto, S. & Matsuoka, T. 1993. A Method for Dynamic Simulation of Rigid and Flexible Fibers in a Flow Field. *J. Chem. Phys.* 98 (1): 644-650

Yu, M., Takach, N.E., Nakamura, D.R. & Shariff, M.M. 2007. An Experimental Study of Hole Cleaning Under Simulated Downhole Conditions. Paper SPE 109840 presented at the SPE Annual Technical Conference and Exhibition, Anaheim, California, 11-14 November.

Zhou, L., Ahmed, R.M., Miska, S.Z., Takach, N.E., Yu, M., & Pickell, M.B. 2004. Experimental Study & Modeling of Cuttings Transport with Aerated Mud in Horizontal Wellbore at Simulated Downhole Conditions. Paper SPE 90038 presented at the SPE Annual Technical Conference and Exhibition, Dallas, Texas, 26-29 September.

Zhu, C. 2005. Cuttings Transport with Foam in Horizontal Concentric Annulus Under Elevated Pressure and Temperature Conditions. Ph.D. Dissertation, University of Tulsa, Tulsa, Oklahoma.
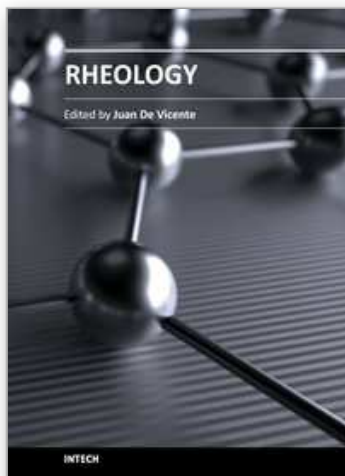
Rheology

Edited by Dr. Juan De Vicente

This book contains a wealth of useful information on current rheology research. By covering a broad variety of rheology-related topics, this e-book is addressed to a wide spectrum of academic and applied researchers and scientists but it could also prove useful to industry specialists. The subject areas include, polymer gels, food rheology, drilling fluids and liquid crystals among others.

How to reference

In order to correctly reference this scholarly work, feel free to copy and paste the following:

Matthew George, Ramadan Ahmed and Fred Growcock (2012). Stability and Flow Behavior of Fiber-Containing Drilling Sweeps, Rheology, Dr. Juan De Vicente (Ed.), ISBN: 978-953-51-0187-1, InTech, Available from: http://www.intechopen.com/books/rheology/stability-and-flow-behavior-of-fiber-containing-drilling-sweeps

INTECH
open science | open minds